

# **Design and Fabrication of PEG and PVA Based Hydrogels for Potential Use as Artificial Vitreous Substitutes**

A DISSERTATION SUBMITTED BY

**REESHA K.V.**

IN PARTIAL FULFILLMENT OF THE REQUIREMENTS

FOR THE AWARD OF

**MASTER OF PHILOSOPHY**



**SREE CHITRA TIRUNAL INSTITUTE FOR MEDICAL  
SCIENCE AND TECHNOLOGY**

**THIRUVANANTHAPURAM**

**INDIA**

**JULY 2016**

## DECLARATION

I, **Reesha K. V.**, hereby certify that I had personally carried out the entire work on depicted in the thesis entitled, “Design and fabrication of PEG and PVA based hydrogels for potential use as an artificial vitreous substitute” for the degree of Master of Philosophy in Polymer Division, Biomedical Technology Wing. Other sources of support and information have been acknowledged in the text. I also declare that the content of this dissertation has not previously submitted for the award of any degree or diploma up to this date.

**Thiruvananthapuram**

**Reesha K. V.**

**Roll No: 160001, 2015/ MPhil/01**

**SREE CHITHRA TIRUNAL INSTITUTE FOR MEDICAL SCIENCES &  
TECHNOLOGY**

**Thiruvananthapuram – 695011, INDIA**

(An Institute of National Importance under Govt. of India)

Phone - (91) 0471-2520248 Fax - (91) 0471-2341814



**CERTIFICATE**

This is to certify that Ms. **Reesha K. V.** submitted her thesis entitled “Design and Fabrication of PEG and PVA Based Hydrogels for Potential Use as Artificial Vitreous Substitutes” is bonafide work done by her in Polymer Division, Biomedical Technology Wing under my supervision in partial fulfillment for the Degree of Master in Philosophy. No part of this embodied matter was submitted for any award of degree or diploma prior to this date.

Place: Thiruvananthapuram

Date:

Dr. M Jayabalan  
Scientist-G & Head  
Polymer Division  
BMT Wing, SCTIMST

The Dissertation entitled

**“Design and Fabrication of PEG and PVA Based Hydrogels for Potential  
Use as Artificial Vitreous Substitutes”**

Submitted by

**Reesha K. V.**

For the degree of

**Masters of Philosophy in Biomedical Technology**

**SREE CHITRA TIRUNAL INSTITUTE FOR MEDICAL SCIENCES &  
TECHNOLOGY, THIRUVANANTHAPURAM – 695011, INDIA**

is evaluated and approved

by

.....

Dr. M Jayabalan Ph.D., D.Sc.,

Scientist G & Head

Polymer Division

BMT wing, SCTIMST

(Research Supervisor)

.....

Examiner's

Name and Designation

## *Acknowledgements*

*I wish to express my heartfelt gratitude and respect to my supervisor **Dr. M. Jayabalan**, Scientist – G & L Head, Polymer Division, BMT Wing, SCTIMST for giving me an incredible opportunity to be part of the lab along with his constant encouragement, guidance, critical evaluations, discussions and fatherly suggestions throughout my M.Phil. programme.*

*I am also highly indebted to my coguide, **Dr. Shivaram Selvam**, INSPIRE Faculty for his guidance and support.*

*My gratitude to **Dr. Sunita Prem Victor**, Scientist – D Adhoc, Polymer Division, for her support. I place my gracious thanks to my lab mates **Ms. Remya** (SRF), **Mr. Adarsh** (Project Assistant), **Mr. Vineeth** (SRF), **Mr. Shamon** (Project Engineer), **Ms. Gayathri** (JRF) for their constant support and encouragement.*

*I convey my indebtedness and gratitude towards, the Previous M.Phil. co-ordinators **Dr. M. Jayabalan**, for his support and valuable suggestions during my initial phase of M.Phil. programme also I acknowledge present M.Phil. co-ordinator **Dr. Manoj Komathi**, **Dr. Maya Nandakumar** for their valuable guidance and support.*

*Heartfelt thanks to all my friends and well wishers who supported me throughout the course. Especially, Riju, Abin, Jimna, Archana, Prabha, Deepa, Lekha, Sneha, Sreelakshmi and all my classmates. Last but not least I thank all the faculty members, technical staff, admin staff and the entire Chitra family for all the learning, fun and joy. I also take the opportunity to thank all the academic staff especially The Head, BMT Wing, Deputy Registrar and The Director, SCTIMST for facilities provided.*

*I am also very much indebted to my family. Words cannot express my indebtedness and deepest sense of gratitude towards my dearest Achan, Amma and brother for their unconditional love, encouragement and emotional support that keep doing well. Lastly, I thank God almighty for enabling me to continue my studies and constantly guiding me through the life.*

*Thiruvananthapuram*

*Reesha K. V.*

# Table of Contents

No.	Page
<b>Chapter I</b>	
<b>INTRODUCTION</b>	1
<b>1. Polymers for medical applications</b>	1
<i>1.1 Synthetic polymeric biomaterials</i>	2
<i>1.2. Degradable polymers for medical applications</i>	4
<i>1.2.1. Hydrolytically degradable polymers</i>	5
<i>Poly glycolide</i>	
<i>Poly lactide</i>	
<i>Polyethers</i>	
<i>1.3. Vitreous substitute</i>	7
<i>1.4. Structure and function of vitreous body</i>	7
<i>1.4.1. Anatomical Properties</i>	7
<i>1.4.2. Chemical Composition</i>	8
<i>1.4.3. Physical properties</i>	9
<i>1.5. Function of native vitreous</i>	10
<i>1.6. Artificial vitreous substitutes</i>	11
<i>1.6.1. Gas based substitutes</i>	11
<i>1.6.2. Expansible Gas-based Substitutes</i>	11
<i>1.6.3. Per fluorocarbon liquid</i>	12
<i>1.6.4. Semi fluorinated alkanes</i>	13
<i>1.6.5. Silicone oil</i>	13
<i>1.6.6. Silicone oil/SFA combinations</i>	14
<i>1.7. Ideal vitreous substitute</i>	15
<i>1.8. Polymeric hydrogels and vitreous characteristics</i>	15
<i>1.8.1 Natural polymeric based vitreous substitutes</i>	15
<i>1.8.2. Synthetic polymeric vitreous substitute</i>	16

## Chapter II

<b>2. OBJECTIVES AND SCOPE</b>	19
--------------------------------	----

## Chapter III

<b>3. EXPERIMENTAL</b>	21
<b>3.1 Materials</b>	21
<b>3.2 Synthesis of Poly (ethylene glycol fumarate) (OPF)</b>	21
<b>3.3 Synthesis of allyl polyvinyl alcohol (APVA)</b>	23
<b>3.4 Preparation of pregel formulation</b>	24
<i>3.4.1 OPF pregel</i>	24
<i>3.4.2 APVA pregel</i>	24
<b>3.5 Preparation of hydrogels</b>	24
<i>3.5.1 OPF based hydrogels</i>	24
<i>3.5.2 APVA based hydrogels</i>	25
<b>3.6 Physicochemical Characterization of prepolymer</b>	25
<i>3.6.1 Nuclear magnetic resonance (NMR)</i>	25
<i>3.6.2. Fourier transform Infrared spectroscopy (FTIR)</i>	26
<i>3.6.3 Gel permeation chromatography (GPC)</i>	26
<i>3.6.4 Determination of Viscosity of pregel formulations</i>	27
<b>3.7. Characterizations of hydrogels</b>	27
<i>3.7.1. Swelling Studies</i>	27
<i>3.7.2 Crosslink Density</i>	28
<i>3.7.3 Mechanical Property</i>	29
<i>3.7.4 Degradation</i>	29
<i>3.7.5 .Surface Morphology</i>	30
<i>3.7.6 Differential Scanning Calorimetry (DSC)</i>	31
<i>3.7.7 Thermogravimetric Analysis (TGA)</i>	31
<i>3.7.8. Contact angle sessile drop method</i>	32
<b>3.8 Optical properties</b>	32
<i>3.8.1 Refractive Index</i>	32
<i>3.8.2 Transparency</i>	33
<b>3.9. Biological Characterization of hydrogels</b>	33
<i>3.9.1 Cytotoxicity assay</i>	33

3.9.2. <i>MTT Assay of polymer resin</i>	33
3.9.3. <i>Direct Contact Assay</i>	34
3.9.4. <i>Live /dead cell assay of direct contact</i>	34
3.9.5. <i>MTT Assay of Hydrogels</i>	35

## **Chapter IV**

<b>4. RESULTS AND DISCUSSION</b>	36
<b>4.1. Synthesis of pregel formulations</b>	36
4.1.1. <i>Oligo polyethylene glycol fumarate oligomer (OPF)</i>	36
4.1.2. <i>Allyl - poly vinyl alcohol</i>	37
<b>4.2. Characterization of pregel formulations</b>	38
4.2.1. <i>Spectral analysis of oligo polyethylene glycol</i>	39
4.2.2. <i>Spectral analysis of Allyl polyvinyl alcohol</i>	40
4.2.3 <i>FTIR analyses of oligo polyethylene glycol fumarate (OPF)</i>	41
4.2.4. <i>FTIR analysis of Allyl poly vinyl alcohol</i>	42
4.2.5. <i>GPC analysis of OPF and APVA</i>	42
4.2.6. <i>Viscosity of pregel formulations</i>	43
<b>4.3. Preparation of Hydrogels</b>	43
4.3.1. <i>OPF based hydrogels</i>	44
4.3.2. <i>APVA based hydrogels</i>	47
<b>4.4 Hydrogel physiochemical properties</b>	49
4.4.1. <i>Swelling studies of OPF hydrogels</i>	49
4.4.2. <i>Swelling studies of APVA hydrogels</i>	50
4.4.3 <i>Crosslinking density and molecular weight between crosslinks</i>	51
4.4.4. <i>Mechanical Property</i>	52
4.4.5. <i>Degradation Studies</i>	53
4.4.6. <i>Surface Morphology</i>	56
<b>4.5 .Thermal properties of hydrogel</b>	59
4.5.1. <i>DSC analysis of hydrogels</i>	59
4.5.2. <i>TG analysis of hydrogels</i>	60
4.6. <i>Contact Angle Measurements</i>	62
<b>4.7. Optical properties</b>	63
4.7.1. <i>Refractive Index</i>	63

4.7.2. <i>Transmittance</i>	64
<b>4.8 In vitro Cytotoxicity</b>	65
4.8.1 <i>MTT Assay of resin</i>	65
4.8.2. <i>Direct Contact Assay</i>	67
4.8.3. <i>Live/Dead cell Assay</i>	68
4.8.4. <i>MTT Assay of prepared hydrogels</i>	70
<b>Chapter V</b>	
<b>5. SUMMARY AND CONCLUSION</b>	72
<b>References</b>	75

## List of Figures

Serial No.	List of figures	Page No
<i>1</i>	Figure 1.1. Transverse section of the eye with an outline of the vitreous body landmarks	<i>10</i>
<i>2</i>	Figure 3.1. Synthesis scheme of oligo polyethylene glycol fumarate	<i>22</i>
<i>3</i>	Figure 3.2. Synthesis scheme of allylpolyvinyl alcohol oligomer	<i>23</i>
<i>4</i>	Fig.4.1.H-NMR spectrum of oligo polyethylene glycol fumarate	<i>39</i>
<i>5</i>	Fig.4.2.H-NMR spectra of allylpolyvinyl alcohol oligomer	<i>40</i>
<i>6</i>	Figure 4.3 FTIR spectrum of oligo polyethylene glycol fumarate	<i>41</i>
<i>7</i>	Figure 4.4. FTIR spectra of allylpolyvinyl alcohol oligomer	<i>42</i>
<i>8</i>	Figure 4.5. Prepared OPF hydrogels	<i>45</i>
<i>9</i>	Figure 4.6. Prepared APVA hydrogels	<i>49</i>
<i>10</i>	Figure 4.7. (a) Weight swelling ratio and (b) Equilibrium water content of the OPF hydrogels (Data represents mean+SD with n=4 samples)	<i>50</i>
<i>11</i>	Figure 4.8. (a) Weight swelling ratio and (b) Equilibrium water content of the prepared APVA hydrogels	<i>51</i>
<i>12</i>	Figure 4.9. Variation of mass (a) and pH (b) of the OPFII hydrogels during aging	<i>54</i>

13	Figure 4.10. Variation of mass (a) and pH (b) of the APVAII hydrogels during aging	55
14	Figure 4.11. Surface morphology of OPFII hydrogels. virgin hydrogel (a), hydrogel after 3 <sup>rd</sup> week of aging (b) and hydrogel after 6 <sup>th</sup> week of aging (c)	57
15	Figure 4.12. Surface morphology of APVAII hydrogels. virgin hydrogel (a), hydrogel after 3 <sup>rd</sup> week of aging (b) and hydrogel after 6 <sup>th</sup> week of aging (c)	58
16	Figure 4.13. DSC curve of hydrogels. (a) OPFII and (b) APVAII.	59
18	Figure 4.14. TG curve of OPFII hydrogel.	61
19	Figure 4.15. TG curve of APVAII hydrogel.	62
20	Figure 4.16. Contact angle measurements. OPFII hydrogel (a) and APVAII hydrogel (b).	63
21	Figure 4.17. Transparency of hydrogels. OPFII (a) and APVAII hydrogel (b).	64-65
22	Figure 4.18. MTT assay of leachable from the OPF pregel solution	66
23	Figure 4.19. MTT assay of leachable from the APVA pregel solution	66
24	Figure 4.20. Cytocompatibility- Direct contact assay of hydrogels. OPFII hydrogel (a), APVAII hydrogel (b) and L929 control cells (c)	67-68
25	Figure 4.21. Cell viability of cells on direct contact with hydrogels. OPFII hydrogel (a), APVA hydrogels (b) L929 Control cells (c) (Ethidium bromide/Acridine orange staining)	69-70

26	Figure.4.22. MTT assay of leachables from the OPFII hydrogel	71
27	Figure.4.23. MTT assay of leachables from the APVAII hydrogel	71

## List of Tables

Serial no	List of tables	Page No
<i>1</i>	Table.1 Main properties and applications of synthetic polymeric biomaterials	<i>3</i>
<i>2</i>	Table.1.1.Biodegradable polymers and their degradation profiles	<i>5</i>
<i>3</i>	Table.4.1. Molecular weight data of oligomers	<i>43</i>
<i>4</i>	Table 4.2 OPF hydrogel formulations and their setting characteristics	<i>44</i>
<i>5</i>	Table 4.3. APVA hydrogel formulations and their setting characteristics	<i>47</i>
<i>6</i>	Table.4.4. Crosslinking density and Molecular weight between crosslinks	<i>52</i>
<i>7</i>	Table 4.5. Mechanical properties of OPF and APVA hydrogels	<i>53</i>
<i>8</i>	Table 4.6. DSC analysis of hydrogels	<i>54</i>
<i>9</i>	Table 4.7. Refractive index of OPFII and APVAII hydrogels	<i>64</i>

## List of Schemes

Serial No	List of scheme	Page no.
<i>1</i>	Scheme 4.1. Schematic representation of synthesis of oligo polyethylene glycol fumarate	<i>37</i>
<i>2</i>	Scheme 4.2 Schematic representation of synthesis of allyl-poly vinyl alcohol.	<i>38</i>
<i>3</i>	Scheme 4.3 Crosslinking of OPF oligomer in the formation of hydrogel	<i>46</i>
<i>4</i>	Scheme 4.4 Crosslinking of APVA hydrogels schematic representation	<i>48</i>

## Abbreviations

APVA	Allyl Polyvinyl Alcohol
DSC	Differential Scanning Calorimetry
kPa	Kilo Pascal
mg	Milligram
ml	Millilitre
OPF	Oligo Polyethyleneglycol Fumarate
PEG	Polyethylene Glycol
PEGDA	Polyethylene Glycol Diacrylate
TEMED	Tetramethylethylenediamine
TGA	Thermogravimetric analysis
VS	Vitreous substitute

# **Chapter I**

## **INTRODUCTION**

### **1. Polymers for medical applications**

For the last few decades, polymers have found extensive applications in the medical field, such as scaffolds for tissue engineering, biosensors, actuators, bio separation devices, reactive coatings, medical imaging, and medical devices. The production of polymers and their preparation in different structures and compositions gives appropriate physiochemical, interfacial and biomimetic properties for specific applications. Polymeric biomaterials have ease of manufacturability and can be molded into films, gels, membranes, sheets, capsules, spheres, particles, 3-D scaffolds. They have good processability, reasonable cost and possess desired mechanical and physical properties<sup>1</sup>.

Polymers are large organic macromolecules consisting of repeating monomeric units. Polymers are formed by monomers which are covalently bonded together by chains of atoms. The entangled chains of the polymer are formed by the weak secondary bonds of attraction between the covalent bonds such as hydrogen and Vander Waals bonds. Polymers show weak thermal and electrical properties due to their covalent interatomic bonding

within the molecules. The molecular weight, chemical side groups, chain structure and composition of backbone are responsible for the mechanical and thermal behavior of polymers.<sup>2</sup>

According to polymerization techniques, polymers can be classified into bulk polymerization, condensation polymerization, and emulsion and suspension polymerization. In bulk polymerization, monomers are reacted with each other using appropriate catalyst and initiators fed in to the reactor without solvent. At the end of the reaction, a solid mass of synthesized polymer being formed. In condensation polymerization different monomer units are condensed to form a polymer with byproducts. The reactions are slightly exothermic and have low viscosity thereby enhancing ready mixing. In solution polymerization, polymerization takes place in a solvent in which both monomers and formed polymers are soluble. In suspension polymerization, the monomer is a dispersed phase in an aqueous medium and the polymer produced from the reactions are formed as a solid dispersed phase. Emulsion polymerization is same as suspension polymerization but differences are that the initiator is dispersed in the aqueous phase compared to suspension and polymer formed is obtained as very small particles.<sup>3</sup>

### ***1.1 Synthetic polymeric biomaterials***

Synthetic polymers have found various applications as biocompatible biomaterials because of their well-known synthesis and moldable properties. Several synthetic materials are already used as medical products such as poly glycolic acid as absorbable sutures and polyurethane in artificial heart. Several synthetic polymeric materials and their applications in the biomedical field are given below. (Table.1)

**Table.1 Main properties and applications of synthetic polymeric biomaterials<sup>2</sup>**

Synthetic Polymer	Main Applications and Comments
Poly(lactic acid), poly(glycolic acid) and their copolymers	Sutures, drug delivery systems and in tissue engineering, biodegradable, regulate degradation time during copolymerization.
Poly(hydroxyl butyrate),poly(caprolactone) and copolymers,poly(alkylene succinate) etc.	Biodegradable. Used as a matrix for drug delivery systems, cell microencapsulation. Used as additives to change the properties of materials by chemical modification, copolymerization and blending.
Polyamides (nylons)	Sutures, dressing, hemofiltration and blending
Polyethylene (low density)	Sutures, catheters, membranes, and surgical treatments
Poly(vinyl alcohol)	Gels and blended membranes for drug delivery and cell immunoisolation
Poly(ethylene oxide)	Highly biocompatible with different polymer derivatives and copolymers used for biomedical applications
Poly(hydroxyethyl methacrylate)	Hydrogels as soft contact lenses, drug delivery, skin coatings and immunoisolation membranes
Poly(methyl methacrylate) and copolymers	Dental implants and bone replacements
Poly(tetrafluoroethylene) (Teflon)	Vascular grafts, clips and sutures, coatings
Polydimethylsiloxanes	As implants in plastic surgery, orthopedics, blood bags and pacemakers
Poly(ortho esters)	Surface eroding polymers. Application include sustained drug delivery and in ophthalmology

Polymers undergo degradation into smaller fragmented chain units followed by mineralization and absorption. The biodegradation process is primarily chemical degradation through hydrolysis. Physical forces such as wetting/drying, cooling, heating helps in the deterioration of the polymer chains which is exacerbated by biochemical agents that come into contact with the polymer surface fulfilling the degradation process.

In medical device applications, polymer degradation often limits the performance of the implanted material. Depending on the application, different products with different degradation rates are required. For example, polymers used as tissue engineering scaffolds should have controllable degradation rate for enhancing tissue regeneration. On the other hand, polymers for bone implants should have good strength and less degradability. Polymers used for drug delivery applications should have tunable degradability ranging between days to months.

### ***1.2. Degradable polymers for medical applications***

A lot of efforts are focused on developing biodegradable materials based on natural and synthetic polymers.<sup>4</sup> Biodegradable natural polymers cause less toxicity and does not evoke significant foreign-body reactions in host tissues compared to synthetic materials. In biomedical applications, notable characteristics are required including, controllable degradability, less inflammatory reactions in host tissues, desired mechanical properties, good sterilizability and process ability.<sup>5</sup>

Biodegradable polymers are composed of hydrolytically and enzymatically degradable polymers. Hydrolytically degradable polymers break down due to their hydrolytically unstable chemical bonds and undergo degradation. Hydrolytically degradable

bonds in polymer chains mainly include esters, anhydrides, acetals, carbonates, amides, and urethanes. Table.1.1 shows biodegradable polymers and their degradation profiles.

**Table.1.1.Biodegradable polymers and their degradation profiles.**<sup>5</sup>

<b>Polymers</b>	<b>Structure</b>	<b>Mw/ kD</b>	<b>Degradation rate</b>	<b>Medical application</b>
Poly(glycolide)	Crystalline	-	100% in 2–3 months	Suture, Soft tissue anaplerosis
Poly(L-lactide)	Semicrystalline	100–300	50% in 1–2 years	Fracture fixation, Ligament augmentation
Poly(ε-caprolactone)	Semicrystalline	40–80	50% in 4 years	Contraceptive delivery implant
Poly(p-dioxanone)	Semicrystalline	-	100% in 30 weeks	Suture, Fracture fixation
Poly(orthoester)	Amorphous	100–150	60% in 50 weeks	Contraceptive delivery implant

### *1.2.1. Hydrolytically degradable polymers*

#### *Poly glycolide*

Polyglycolides (PGA) are ester family of polyesters having an aliphatic bond in their back bone. PGA is the first degradable polymer investigated for medical use. It has a melting point at 200 °C and glass transition temperature of 35-40 °C. PGA is used as a

degradable suture, DEXON<sup>®</sup>, from 1970s. It is mainly used in short term tissue engineering applications.

### *Poly lactide*

Poly lactide is a naturally occurring polymer from lactic acid monomers. Poly lactides include poly(L-lactic acid) (PLLA), poly(D-lactic acid) (PDLA), and poly(D,L-lactic acid) (PDLLA), a racemic mixture of PLLA and PDLA, have been extensively used for various applications. PLLA has melting point of 175 °C and glass transition of 60 - 65°C. It is used as bone fixator and as tissue engineering scaffolds for bone applications.

### *Polyethers*

Most of the biomedical research with synthetic polyethers focus on the use of poly(propylene glycol) (PPG) and poly(ethylene glycol) (PEG). Polyethers have good stability and they do not readily undergo hydrolytic degradation. Polyether with lower molecular weight is used for biomedical applications because of its lower accumulation of degradation product compared to higher molecular weight polyethers. PEG based hydrogels have been used as in situ-forming injectable hydrogels. It has also been tested in formulations for intravitreal drug delivery, repair of scleral incisions and sealing retinal detachments. For example, 5 wt% PEG in phosphate-buffered saline have been administrated as artificial vitreous substitutes (VS). The injected VS had good mechanical and optical properties similar to the natural vitreous and was well tolerated by the retina with minimal histological electrophysiological changes during the rabbit implanted studies.<sup>6</sup>

### ***1.3. Vitreous substitute***

Retinal detachment is a significant cause of vision loss. Recently, efforts have been undertaken for the development of innovative approaches in vitreo retinal treatments. Vitreous humor is a gelatinous structure that fills the space between the lens and the retina<sup>7</sup> and is composed of 98 - 99% water by weight. The human vitreous is composed of collagen fibers and hyaluronic acid and hence is a natural polymeric hydrogel.<sup>8</sup> The vitreous is the largest part of the eye by volume and plays an important role in the support and growth of its structures. The retinal pigment epithelium (RPE) is dependent on the vitreous hyaluronic acid composition<sup>9</sup>. The vitreous is a highly transparent substance that transmits 90% visible light and gives support to lens capsule.<sup>10,11</sup> Vitreous humor helps in the circulation of metabolites throughout the eye and decreases lens exposure to oxygen.<sup>12</sup>

### ***1.4. Structure and function of vitreous body***

#### ***1.4.1. Anatomical Properties***

Vitreous humor consists of several parts with different densities and biochemical compositions so it is not homogeneous. The vitreous cortex is closest to the retina and is also the denser part of the vitreous with variable thickness.<sup>13</sup> Vitreous is overlying the vitreous base which is denser than the cortex, also called as ora serrata. Vitreoretinal interface is a membrane complex seen between border of vitreous and retina. It is comprised of internal limiting membrane of the retina (ILM) and a layer of dense collagen fibers adjacent to the ILM<sup>14</sup>.

#### *1.4.2. Chemical Composition*

Vitreous body contains 98% weight is water, but is not in free form as some of it is bound to proteins and glycosaminoglycans.<sup>15</sup>

*Proteins:* The content of proteins in the vitreous is small when compared to the size of the vitreous body. The vitreous synthesizes transferrin and iron-binding proteins which gives a protective effect towards small vitreal hemorrhages.<sup>16</sup> The most abundant insoluble collagen concentration in vitreous is ~300µg/ml and is found in the form of type II (60-70%), type IX (25%), type V/XI (10-25%) and type IV (<10%) collagen.<sup>17</sup>

*Glycosaminoglycan:* It is an important constituent of the vitreous, and is present as hyaluronic acid (HA), chondroitin sulfate (CS) and heparin sulfate. Hyaluronic acid determines the viscosity of the vitreous body and serves as a template for assembly of other extracellular matrix.<sup>18</sup> Chondroitin sulfate in vitreous is in the form of two proteoglycans, versican and type IX collagen. A small percentage of heparin sulfate is present in the vitreous and is presumed to maintain adequate spacing between the collagen fibrils.

*Metabolites:* The major metabolites, glucose and lactic acid, are found in vitreous and is needed for support of enzymatic activity. The concentration of glucose is found to be half that in plasma for most species.

*Ascorbic acid:* Ascorbic acid found in vitreous body is higher than in plasma and is associated with the process of liquefaction during aging. Recent studies have showed that it plays an important role as a potent antioxidant and prevents early cataract formation.<sup>12</sup>

*Amino acids:* Amino acids concentration in the vitreous is similar to those in plasma.

*Fatty acids:* The total lipid concentration in the vitreous is stable with age and unsaturated fatty acids constitute around 50-55%<sup>19</sup>.

*Prostaglandins:* Prostaglandins are a group of physiologically active lipid compounds composed of unsaturated carboxylic acids. The human vitreous contains~ 100 g/ml of prostaglandins.

*Cells:* Three types of cells are mainly identified in vitreous body. They are hyalocytes, fibrocytes and macrophages. Hyalocytes are located on the vitreous surface adjoining the retinal ILM. Fibrocytes help in the secretion of collagen and macrophages are also involved in phagocytosis.<sup>20</sup>

#### *1.4.3. Physical properties*

*Organization:* The long chain collagen fibrils and hyaluronic acid molecules makes the vitreous gelatinous and provides it with viscoelastic properties.<sup>21</sup>

*Gradients:* The vitreous contains several compositional gradients including collagen, protein, bound water, HA, glucose, lactate and oxygen. A small pressure gradient also helps in the movement of ions. The standing potential of eye is fortified by the gradients and constant movement of ions. Gradients in anterior and posterior of the eye part is much more viscous and denser<sup>22</sup> compared to the middle segment of the eye.

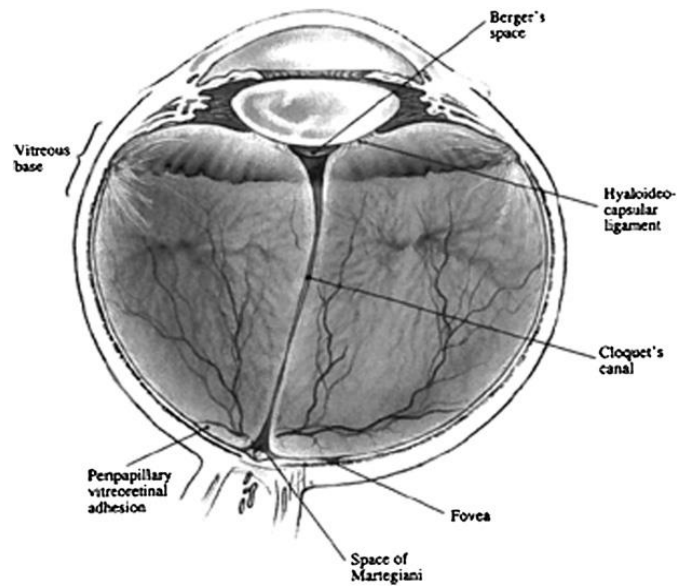


**Figure1.1.** Transverse section of the eye with an outline of the vitreous body landmarks.<sup>23</sup>

### ***1.5. Function of native vitreous***

The vitreous plays an essential role in the growth of RPE. Hyaluronic acid in vitreous plays a role in sustaining internal pressure within the eye.<sup>24</sup> The high HA content in the vitreous protects the eye from low frequency mechanical stress and vibration. HA behaves as viscoelastic body rather than a viscous liquid thereby acting as shock absorber of the eye. The highly transparent ocular medium that transmit 90% visible and near infrared light also acts as a support for the lens capsule.<sup>10</sup> The vitreous acts as a barrier to biochemical substances and cells thereby inhibiting proliferation, inflammation and neovascularization. Vitreous helps in the metabolism of the surrounding tissue by transporting essential molecules and minimizes the risk of cataract formation by protecting the lens from oxidative damage.<sup>12</sup>

As age increases, the vitreous undergoes liquefaction which affects normal vision.

Vitreous liquefaction causes retinal detachment, a condition where the neurosensory retinal segments separate from posterior part of the eye, which leads to dangerous eye complications such as macular hole, vitreous hemorrhage, vision loss, etc.<sup>25</sup> To treat this condition, vitrectomy, a surgical procedure which involves the removal of the vitreous in the central cavity of the eye and replacing with an artificial substitute, is performed. Currently used vitreous substitutes have the ability to reproduce some of the important characteristics of native vitreous.

### ***1.6. Artificial vitreous substitutes***

There are several types of VS currently available. These include gases (air, expansile gases), liquids (perfluorocarbon liquids) and polymers.

#### *1.6.1. Gas based substitutes*

*Air-based substitutes:* In 1911 Ohm first used air as VS for retinal detachments. Cheaply and readily available air can easily absorb by eye and replaced by aqueous humor. Air based materials have short residence time and hence have limited use as a vitreous substitute.

#### *1.6.2. Expansible Gas-based Substitutes*

Sulfur hexafluoride (SF<sub>6</sub>) and perfluoropropane are heavier than air and are commonly used as VS. Both are colorless, odorless, non toxic and are used in non-expansile concentrations to fill the vitreous cavity.

### *1.6.3. Per fluorocarbon liquid*

The more ideal vitreous substitute is a liquid or gelatinous solid that can respond to head movement and maintain tamponade effect without being absorbed or degraded. Water and balanced salt solutions were the first liquids used as VS.<sup>26</sup> In 1990s, modern liquid substitutes such as perfluorocarbon liquids (PFCLs) were investigated. PFCLs are synthetic, fluorinated, carbon containing compounds with clear, colorless, and odorless characteristics. They possess an extensive capacity for transporting and releasing both O<sub>2</sub> and CO<sub>2</sub> and is twice denser than water.<sup>27</sup> They have good oxygen carrying capability and was originally designed as blood substitutes.<sup>28</sup> The most commonly used PFCLs are perfluorodecalin (PFD), perfluorohexyloctane (F6H8), perfluoroperhydrophenanthrene, and octafluoropropane.

*Use:* PFCLs could potentially be used as long-term tamponade of inferior retinal detachments by virtue of being heavier than water. In complex retinal detachments PFCLs are used intraoperatively to temporarily flatten the retina and are used as replacement for silicone oil or another long-term substitute. However, they are currently limited by long-term toxicity.

*Advantages:* PFCL's high specific gravity makes them useful for the intraoperative repair of complex retinal tears. The intraoperative removal of PFCLs gives peculiar complications in anterior and posterior segments.<sup>28</sup> The high oxygen solubility of PFCL's provides good neuroprotective effect on ischemic retina<sup>29</sup>.

*Disadvantages:* PFCL's are intraoperatively limited because of their long-term toxicity. Disorganization of retinal cell growth pattern, neuritis, and other toxic effects are showed by PFD and perfluoroperhydrophenanthrene in in vitro experiments.<sup>30</sup>

#### *1.6.4.Semi fluorinated alkanes*

Semifluorinated alkanes are also known as partially fluorinated alkanes. It is the first tamponade agent used for intraoperative setting and is heavier than water.<sup>31</sup> It have low specific gravity, 1.35 g/mL, compared to PFCLs with a refractive index of 1.3.

Use: In earlier days, SFAs were used as a solvent for silicone oil and was temporarily used as endotamponade for special cases of retinal detachment when silicone oil did not offer desired results.

*Disadvantage:* It is associated with cataract formation, emulsification followed by the presence of soft epiretinal membranes.

#### *1.6.5.Silicone oil*

In 1960s silicone has been used as a VS. Its structure is similar to that of silicone rubber but shorter polymer chains and absence of crosslinking makes it exist as a liquid form. It has hydrophobic characteristics with a specific gravity of 0.97 g/mL and refractive index of 1.4.

*Use:* It is the currently accepted vitreous substitute for long term application. It is available in many viscosity variants which is measured in centistokes. Clinically 1000 to 5000 centistoke silicone oils (SO) are used now. SO are typically removed after 3-6 months.

*Advantages:* SO is very good VS because of its high surface tension, low toxicity, ease of removal and transparency. It possesses 70% anatomical integrity due to its immiscible characteristics with water which gives it high surface tension and low specific gravity. Difficulties in post operative positioning with SO in children and adult is very less so it is a versatile tamponade agent for VS.

*Disadvantages:* SO can undergo traction because it can pass through retinal breaks due to low surface tension property. SO need optimal adjustments due to its refractive index value close to 1.4. Post-operatively, SO shows oil emulsification, incidence of corneal abnormalities at 24 months, which did not differ significantly from sulfur hexafluoride gas, and has been reported to cause problems with both native and implanted lenses

#### *1.6.6. Silicone oil/SFA combinations*

One of the clinically approved tamponade agent for the vitreous is silicone oil/SFA combination. The combination of both mixture gives the advantages of both liquids such as high specific gravity of SFAs and high viscosity of silicone oil making it a good VS with low emulsification. The solubility of this mixture called heavy silicone oils can produce a homogeneous clear solution and varies with the ratio of liquids. The percentage of SO is kept as lower to avoid toxicity.

### ***1.7. Ideal vitreous substitute***

The currently used clinically approved vitreous tamponade have many drawbacks. According to Chirila et al, the ideal VS should have transparency and clarity, biological & chemical inertness, refractive index and density equal to that of the natural vitreous, sufficient rigidity to act as tamponade agent, ability to allow transfer of metabolites, non-absorbable and non-biodegradable characteristics and should have storable, sterilizable, viscoelastic properties.<sup>32</sup>

### ***1.8. Polymeric hydrogels and vitreous characteristics***

Polymeric hydrogels are wet and soft materials that are composed of three dimensional hydrophilic network structure containing large amount of water (50–90%)<sup>33</sup>. Hydrogels are convenient materials for biomedical applications as they are soft materials with hydrophilic and porous nature whose stiffness can be tailored depending on the application.<sup>34</sup>

Injectable hydrogels are excellent biomaterials for tissue engineering applications as they possess good biocompatibility, easily controllable physical properties, minimally invasive delivery and undergo solution to gelation (sol-gel) transition in situ through physical or chemical stimuli.<sup>35</sup>

#### ***1.8.1 Natural polymeric based vitreous substitutes***

Collagen based semisynthetic polymer VS were used during the early days of vitrectomy. Kurt *et al* reported that tropocollagen isolated from calf skin offered clear,

stable hydrogels with properties close to native vitreous when implanted in rabbit and monkey model.<sup>36</sup> Pruett *et al* evaluated proctase-treated collagen VS but the gel lacked rigidity.<sup>37</sup> An alkaline-solubilized collagen with hyaluronic acid VS in rabbit model revealed no adverse effect on ocular tissues with increased collagen half-life was reported by Nakagava *et al*.<sup>38</sup> Recently Lai *et al* developed a chemically modified gelatin hydrogels by crosslinking it with glutaraldehyde (GTA) and ethyl dimethyl amino propyl carbodiimide (EDC). In vivo studies in rabbit model exhibited good biocompatibility in EDC cross-linked gelatin gels.<sup>39</sup> Commercially available sodium hyaluronidate showed excellent biocompatibility and tolerance in ocular tissues but due to its short residence time in vitreous cavity and poor tamponade effect it was unsuitable to serve as an ideal VS.<sup>40</sup> Surie *et al* formed a gellan gum gel at RT and their structure was maintained in body temperature. In vitro studies on mouse fibroblasts showed excellent biocompatibility but poor rheological properties than that of natural vitreous. However, mechanical properties was improved by adding CaCl<sub>2</sub> to the gellan gum/HA mixture.<sup>41</sup>

### *1.8.2. Synthetic polymeric vitreous substitute*

There are several synthetic polymeric materials that show promise as good VS. Current research is increasingly focusing on synthesizing highly biocompatible polymers that might be able to mimic the functional properties of the natural vitreous, rather than its physical characteristics. Poly(2-hydroxyethyl methacrylate) (PHEMA) is a solid hydrogel that was well-tolerated by ocular tissues and did not elicit retinal damages without undergoing bioabsorption or biodegradation. However, PHEMA implantation required difficult surgical procedures and therefore, was no longer investigated.<sup>42</sup> Polyvinyl alcohol (PVA) also shows great promise as an artificial VS. Maruoka *et al* developed an autoclaved PVA hydrogels and tested in a monkey's eye. These hydrogels showed good optical

properties and long-term biocompatibility.<sup>10</sup> Recently, Cavalieri *et al* studied poly(vinyl alcohol methacrylate) (PVA-MA) hydrogels. The polymer contained a photo initiator that could form a 3-D gel network by irradiating with light at 365 nm. The crosslinking density can be varied by adjusting photo initiator concentration and the radiation exposure time to form in situ gelification. In vitro test showed that hydrogel degradation occurred in the presence of low degree of crosslinking indicating that suitable hydrogels would be those synthesized at high polymer concentrations and with high degree of cross-linking. However, such gels were found to be significantly stiffer than natural vitreous. Nevertheless, PVA-MA hydrogels offers promise for long-term VS application.<sup>43</sup>

Hydrogels offer great potential for the development of an artificial VS, however, their drawbacks such as short residence time and uncontrolled biodegradation in vivo limits their application. Several researchers are focused on clinically utilizable hydrogel preparation for vitreous substitutes. Feng *et al* developed a novel approach of using foldable capsular vitreous body (FCVB) injected with PVA hydrogel as VS. These crosslinked hydrogels were formed using gamma irradiation and they exhibited good rheological and physical properties with no potential toxicity in vitro. After 180 days retention, 3% PVA hydrogels inside FCVB remained transparent, had good elasticity, minimal biodegradation, good biocompatibility and retina support.<sup>44</sup>

Stimuli-responsive hydrogels have achieved notable consideration due to their manifold applications. These hydrogels shrink or expand or switch between sol to gel state in response to the environmental changes like pH, temperature, or light. Smart hydrogel can be prepared, stored and injected in solution state and undergo in situ gelation via external stimuli. For example, vitreous Pluronic F127<sup>45</sup> ocular and WTG-127<sup>46</sup> have been attempted for use as artificial VS. However, F127 was found to cause severe retinal toxicity and

WTG-12 exhibited a short degradation time and tendency to drift under retinal tears before complete gelation.<sup>47</sup> Work is ongoing to prepare smart hydrogels that not only mimic the optical and rheological properties of the natural vitreous but also bring in antifouling properties and ease of application. Lirong *et al* developed a hydrogel using inexpensive commercially available components: polyethylene glycol acrylate and dithiothreitol. The prepared PEG hydrogels have a compressive modulus of up to 104 Pa and comprised of 87.5% water making their mechanical performance comparable to cross-linked PEG gels. Furthermore, the dynamic nature of the boronate ester linkages imparted the hydrogel with self-healing properties and the gels can be healed within 30 min without external stimulus<sup>48</sup>

## Chapter II

### OBJECTIVES AND SCOPE

The removal of the natural vitreous from the eye during vitrectomy and the loss of vision associated with retinal detachment after vitrectomy are major complications in the area of ophthalmology. The development of an artificial vitreous is greatly needed to fill the role as a tamponade agent to prevent retinal detachment in the posterior part of the eye. Many materials have been developed and used for last few years; but none possess the ideal characteristics of the natural vitreous due to their short term lifetime and biocompatibility issues.

The objectives of this study were to design transparent, injectable pregel formulations that can crosslink via free radical polymerization using a PEGDA as crosslinker and form crosslinked hydrogels *in situ*. Toward this end, we have synthesized two injectable pregel polymer solutions based on polyethylene glycol and polyvinyl alcohol as main polymer chain units. We have introduced fumarate groups in PEG backbone and allyl functional groups in PVA chain to yield a crosslinked hydrogel. The physicochemical properties, optical characteristics, degradation profiles and biological studies of the prepared PEG and PVA hydrogels were evaluated and detailed below.

### **Main objective of the study include**

- ❖ Synthesis and characterization of oligo polyethylene glycol fumarate (OPF) and allyl functionalized polyvinyl alcohol (PVA) oligomers
- ❖ Characterization of prepared hydrogels by studying the swelling, degradation, mechanical and optical properties
- ❖ Evaluation of cytocompatibility of hydrogels

## Chapter III

### EXPERIMENTAL

#### 3.1. Materials

PEG (Poly ethylene glycol, MW: 600) and fumaryl chloride were purchased from Merck (India). Potassium carbonate, dichloromethane, polyvinyl alcohol (Mw = 18,000), allyl bromide, sodium hydroxide, ammonium persulphate, tetramethylethylenediamine (TEMED), and polyethylene glycol diacrylate (PEGDA, MW: 700) were acquired from Sigma (Bangalore, India). High glucose Dulbecco's Modified Eagle's Medium (DMEM), fetal bovine serum (FBS) and 100X antibiotic-antimycotic solution were obtained from Invitrogen (India). MTT (3-(4,5-dimethylthiazol-2-yl)-2,5-diphenyltetrazolium bromide) assay kit procured from Invitrogen.

#### 3.2. Synthesis of poly (ethylene glycol fumarate) oligomer (OPF)

The oligo polyethylene glycol fumarate (OPF) was synthesized using the experimental setup as shown below (Figure 1). Dried PEG, fumaryl chloride, potassium carbonate ( $K_2CO_3$ ) were measured out in a 1:1:1.5 molar ratio. PEG was dissolved in a

methylene chloride (1:2 v/v) and placed in a two neck flask along with powdered  $K_2CO_3$ . The mixture was stirred with an magnetic stirrer to form a slurry to which fumaryl chloride dissolved in methylene chloride (1:1 v/v) was added dropwise. The reaction mixture was maintained at room temperature (RT) for 50°C for 12 h under reflux using a condenser under nitrogen atmosphere. After polymerization for 12 h the reaction was cooled down and transferred to centrifuge tubes and centrifuged for 15 min at 3000 rpm until potassium chloride (KCl) and unreacted  $K_2CO_3$  were pelleted out. The supernatant was then added drop wise to petroleum ether to extract the oligomer and rotary evaporated to yield a light yellow viscous product.<sup>49</sup>

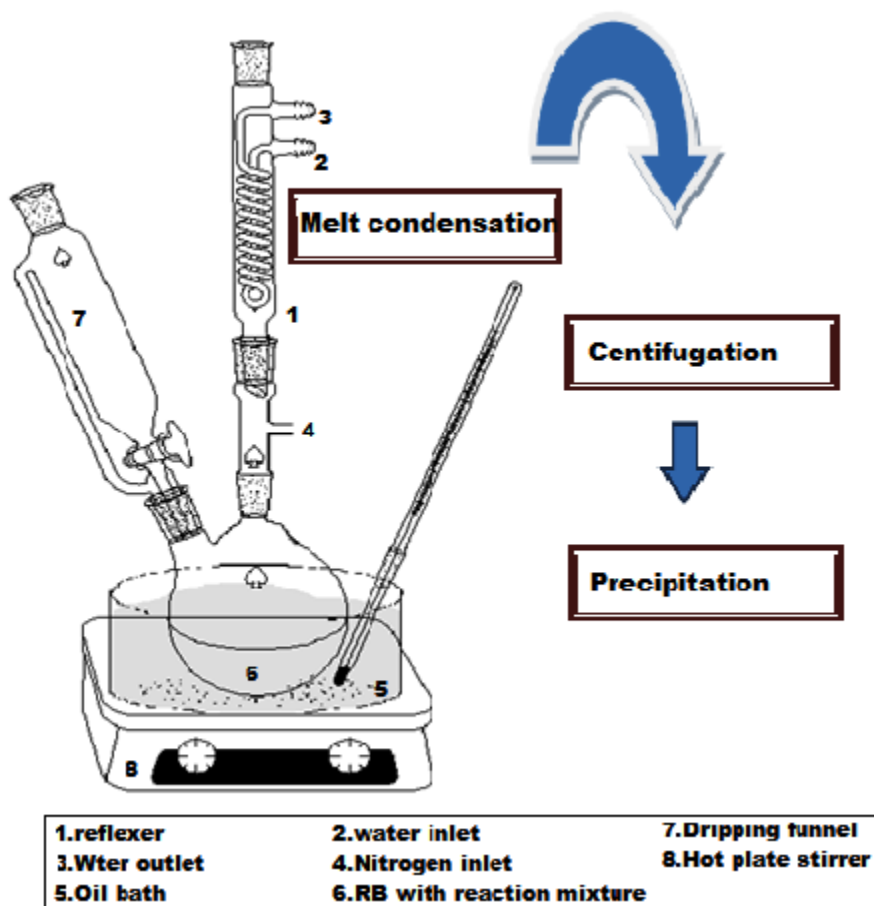


Figure 3.1. Synthesis scheme of oligo polyethylene glycol fumarate

### 3.3. Synthesis of allyl polyvinyl alcohol (APVA) oligomer

APVA was synthesized using the experimental setup as shown below (Figure 2). Three grams of PVA were dissolved in 70 ml water at boiling temperature. To the solution cooled at room temperature was added 30 ml of 0.013 mmol sodium hydroxide followed by the addition of 10 ml of allyl bromide. The reaction mixture was stirred 20 h at 85°C temperature. After 20 h, the obtained pale yellow resin was dialyzed and lyophilized to get a yellow resin which was stored under 4°C.

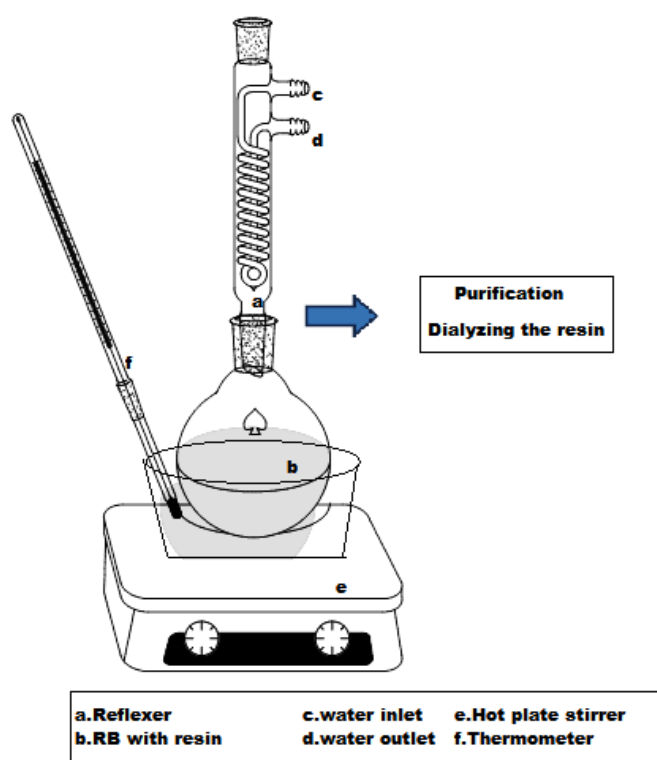


Figure.3.2. Synthesis scheme of allyl polyvinyl alcohol

### **3.4. Preparation of pregel formulation**

#### ***3.4.1 OPF pregel***

Briefly, 0.3 g OPF resin was dissolved in 1 ml of distilled water. The mixture was then gently neutralized with sodium hydroxide solution (2 M) to bring pH to 7.4. The pregel solution was then mixed thoroughly and was used as the working solution.

#### ***3.4.2 APVA pregel***

Briefly, 0.1 g APVA resin was dissolved in 1 ml of hot distilled water. The pregel solution was mixed thoroughly and was used as the working solution.

### **3.5. Preparation of hydrogels**

#### ***3.5.1 OPF based hydrogels***

For the preparation of OPF hydrogel, 400  $\mu$ l of this pregel solution was added to a well of a 48-well tissue culture plate and added 12 mg of PEGDA crosslinker and then polymer crosslinking was initiated by adding the redox initiators, APS (24  $\mu$ L, 2 M) and TEMED (8  $\mu$ L, 6 M) was mixed thoroughly. After 15 min, the disc-shaped hydrogels (12 mm diameter and 3.5 mm height) were scooped out using a clean spatula and were subsequently used for various characterization studies. Three different hydrogels with 6 mg, 12 mg and 16 mg concentration of PEGDA crosslinker were prepared for initial optimization of gel setting and characterization.

### ***3.5.2 APVA based hydrogels***

For the preparation of APVA hydrogel, 400  $\mu$ l of this pregel solution was added to a well of a 48-well tissue culture plate and added 12 mg of PEGDA crosslinker then polymer crosslinking was initiated by adding the redox initiators, APS (24  $\mu$ L, 2 M) and TEMED (8  $\mu$ L, 6 M) was mixed thoroughly. After 2 min, the disc-shaped hydrogels (12 mm diameter and 3.5 mm height) were scooped out using a clean spatula and were subsequently used for various characterization studies. Three different hydrogels with 10 mg, 12 mg and 16 mg concentration of PEGDA crosslinker were prepared for initial optimization of gel setting and characterization.

## **3.6 Physiocochemical characterization of prepolymer**

### ***3.6.1 Nuclear magnetic resonance (NMR)***

Nuclear magnetic resonance (NMR) spectroscopy is a strong analytical technique used for the determination of molecular structure and purity of the material. The principle behind NMR is that the nuclei of atoms have spin and are electrically charged. When an external magnetic field is applied, an energy transfer from base energy to a higher energy level takes place at a wavelength that corresponds to radio frequencies and energy emitted when the spin returns to its base level is of the same frequency. The signal that matches this transfer is measured in many ways and processed in order to yield an NMR spectrum for the nucleus concerned. The NMR analysis of samples were done using Bruker 500 MHZ spectrometer (Bruker Biospin, Billerica, MA) with DMSO as solvent

### ***3.6.2. Fourier transform Infrared spectroscopy (FTIR)***

FTIR spectroscopy is a sensitive technique to determine the functional group analysis of unknown compounds. In FTIR, when infrared radiation is passed through a sample, some of the incident infrared radiation is absorbed by the sample and some are transmitted resulting in a spectrum that gives the molecular absorption and transmission of the sample. This spectrum gives the molecular spectroscopic finger print of the sample.

The synthesized polymer's functional groups were determined using a JASCO FT/IR-4200 spectrometer that included JASCO'S proprietary spectra Manager TM II cross platform software. The FTIR spectrum was recorded by sandwiching samples between two potassium bromide pellets and scanned in the range from 4000 –400  $\text{cm}^{-1}$  at a resolution of 4  $\text{cm}^{-1}$ .

### ***3.6.3 Gel permeation chromatography (GPC)***

GPC is a chromatographic technique for analyzing molecular weight of polymers. Chromatography systems rely on pumps to pass a pressurized liquid solvent containing a sample mixture through a column filled with a solid adsorbent material. Each component in the sample interacts slightly differently with the adsorbent material thereby causing a shift in flow rates for the different components which lead to the separation of the components as they flow out the column. Particles are eluted based on the pore size of the adsorbent material and volume of sample injected into the column. In general, low molecular weight polymers have longer retention times compared to high molecular weight polymers. Molecular weight of the sample was determined using the Waters GPC system 600 series pump with waters Styragel column (HR5E/4E/2/0.5). Five milligram samples were

dissolved in tetrahydrofuran for OPF and THF was used as mobile phase with flow rate of 1 ml/min. For APVA, samples were dissolved in distilled water and sodium nitrate was used as mobile phase with flow rate of 1 ml/min. Waters ultrahydrogel columns 2000/1000/500 with series were used. Dextran and PEG were used for relative calculation.

#### ***3.6.4. Determination of Viscosity of pregel formulations***

The viscosity of pregel formulations of oligomer was determined using a rotational viscometer (RVA-Starch Master 2, Newport Scientific). The polymer was dissolved in water at 37°C and viscosity was measured at 200 rpm as per machine guidelines. Hydrogel pregel formulations of 25 ml was directly put in to the constant stirring using a rotational viscometer (RVA StarchMaster 2, Newport Scientific) and measure the viscosity at 37°C, and 200 rpm for 15 min.

### **3.7. Characterizations of hydrogels**

#### ***3.7.1. Swelling Studies***

Swelling studies were performed to evaluate the water absorbing capacity of hydrogels. Hydrogels were freeze-dried using a lyophilizer. The freeze-dried weight of sample was measured and the hydrogels were incubated in either (PBS, pH~7.4) or water for 24 h at 37°C. After 24 h incubation, the sample wet weight was measured and the weight swelling ratio and equilibrium water content of each sample was calculated according to the following equation.

$$\text{Weight swelling ratio} = W_w / W_d$$

$$\text{Equilibrium water content (EWC)} = \frac{(W_w - W_d) \times 100}{W_w}$$

where,  $W_d$  is the weight of the freeze-dried hydrogel and  $W_w$  is the weight of the wet hydrogel incubated in PBS or water.

### 3.7.2 Crosslink Density

The crosslink density and number average molecular weight between crosslinks of hydrogels were determined. The prepared hydrogels were freeze-dried and their weight was measured. The diameter and thickness of the dried sample was measured using digital vernier calipers. The pre-weighed dried gels were incubated in water for 24 h in 37°C. After 24 h incubation the sample wet weight was measured. Modified Florry-Rehner's equation was used for the calculation of the above parameters.<sup>50</sup>

$$\text{Crosslink density} = \frac{[V_r + \chi V_r^2 + \ln(1 - V_r)]}{\nu_r V_0 (V_r^{\frac{1}{3}} - \frac{V_r}{2})}$$

$$\text{Molecular weight between crosslinks, } M_c = \frac{1}{\zeta}$$

where,  $\chi$  is the Huggin's polymer-solvent interaction coefficient, assumed to be 0.34 and  $V_r$  is the volume fraction of the polymer in water-swollen hydrogel, which can be calculated from the swelling coefficient,  $\Phi$  using the relation,

$$V = \frac{1}{1+\Phi}$$

$$\Phi = \frac{W_s}{W_p} \times \frac{D_p}{D_s}$$

where,  $W_s$  is the weight of the solvent in the swollen polymer,  $W_p$  is the weight of the swollen hydrogel,  $D_p$  is the density of hydrogel,  $D_s$  is the density of water and  $d_r$  is the density of the polymer. The number average molecular weight between crosslinks (MC) was calculated as the reciprocal of crosslink density ( $\text{mol cm}^{-3}$ ).

### ***3.7.3 Mechanical Property***

Hydrogels were prepared in circular plastic mold with 1 cm height and 1 cm diameter with different concentration of crosslinker. The samples were lyophilized and incubated in water for 24 h at 37°C. After swelling, the height and diameter of the sample was again measured using digital vernier calipers. Compression test was carried out in an Instron instrument (model 2510-104) with a 500 N load cell and crosshead speed of 5  $\text{mm/min}^{-1}$  at RT with samples compressed to 60% of their thickness. Compressive stress, load at break and Young's modulus were calculated using Instron's proprietary Bluehill 3 software.

### ***3.7.4 Degradation***

The degradation studies of lyophilized samples were carried out in PBS (pH~7.4) by aging at 37 °C for 7, 14, 21, 28 and 35 days of incubation. Disc shaped hydrogels with 6 mm diameter and 3 mm height were prepared. Gels were incubated in PBS and placed in a orbital shaker under constant agitation of 100 rpm with temperature set to 37 °C. At each time point, the change in pH of the medium was recorded using a pH meter (Cyber scan pH 510, Eutech instruments); the hydrogels were removed, lyophilized and weighed. The weight loss of hydrogels was calculated using the equation below.

$$\text{Mass loss(\%)} = \frac{(M_t - M_o) \times 100}{M_o}$$

Where,  $M_o$  is the initial mass of the hydrogel and  $M_t$  is the mass of the hydrogel at various time points.

### ***3.7.5 .Surface Morphology***

Scanning Electron Microscopy (SEM) is a versatile methodology for analyzing the surface morphology of the material. It helps observe the minute details related to the material's surface characteristics and corresponding pore sizes. SEM provides high resolution images by using electron beams instead of light waves. SEM uses vacuum atmosphere in a column that contain electron guns which emits beams of high energy electrons. The electron beams travels downwards, pass through a series of lenses and focuses on the sample. The kinetic energy carried by accelerated electrons interact with the sample which in turn produces various signals and secondary electrons that are detected by detectors.

Surface morphology and pore size distribution of the hydrogel were recorded using an environmental scanning electron microscope (ESEM). The analysis was performed on lyophilized samples at different time points (days 0, 21 and 42) and visualized under low vacuum conditions (FEI, Quanta 200, USA).

### 3.7.6 Differential Scanning Calorimetry (DSC)

Differential scanning calorimetry is a thermoanalytical technique in which the difference in the amount of heat required to increase the temperature of a sample and reference are measured as a function of temperature. DSC gives the glass transition temperature, melting point, phase transformation information of the samples. The transition of water content in the hydrogels was measured using Differential scanning calorimeter (DSC Q20 V24.4 Build 116, TA Instruments). The lyophilized hydrogel samples of OPF and APVA were swelled in distilled water for 24 h. From that 5 mg samples were cooled to -50 °C and heated to 100°C at a heating rate of 5 °C/min in a nitrogen atmosphere. An empty aluminum pan was used as reference. The ratio of endothermic heat flow of hydrogel to the endothermic heat flow of pure water (334 J/g) gives the freezable water content in the hydrogel. The non-freezable water content (NBW) was obtained from the subtraction of free water (FW) content from the equilibrium water content (EWC).

$$\text{Freezable water content(FW or FBW)} = \frac{\text{Enthalpy of melting endotherm}}{\text{Enthalpy of melting pure water}} * 100$$

$$\text{NBW} = \text{FW} - \text{EWC}$$

### 3.7.7 Thermogravimetric Analysis (TGA)

Thermogravimetric analysis (TGA) is used to measure the thermal properties of the material. TGA is the measure of weight change of material as a function of temperature under nitrogen or helium atmosphere. It gives temperature and weight change of decomposition reactions and often allows quantitative composition analysis. The thermal behavior of the OPF and APVA hydrogels were determined by using TGA (TG, SDT-

Q600, TA, USA) at a heating ramp rate of 10 °C /min. The TGA trace was obtained in the range 40–1000 °C under nitrogen flow using a platinum crucible.

### ***3.7.8. Contact angle sessile drop method***

Contact angle of hydrogels were measured by sessile drop method. Thin films of hydrogels were prepared and dried under RT. Surfaces were appropriately cleaned just before contact angle measurements. The specimen was placed in a measuring cell partially filled with deionized water and covered to initiate saturation of phases. The syringe filled with the deionized water was taken and a small drop was deployed onto the specimen surface with the needle located in the apex of the deposited drop. The contact angle values were measured using a contact angle system (OCA-15 plus, optical contact angle system).

## **3.8 Optical properties**

### ***3.8.1 Refractive Index***

Optical properties are important for hydrogels for use as VS. Refractive index is a measure of velocity of light through vacuum to the velocity of light through medium. It is a fundamental property of material which is useful for calculating the purity of material for optical applications. The freshly prepared OPF gels and APVA gels are incubated in PBS for 24 h. The refractive index of the incubated gels was measured on a J357 Refractometer (Rudolph Research Analytical, Hackettstown, NJ) using a standard protocol.

### **3.8.2 Transparency**

Transparency is the physical property of the material that allows light to pass through the material without being scattered. Transmittance is the ratio transmitted light to that of incident light. It is expressed as percentage of light transmitted. The transmittance of OPF gels and APVA gels were measured by UV-visible spectrophotometer (Shimadzu, Model UV-1800,240 V, Japan) between 400 nm to 800 nm in water at 25 °C. The measured absorbance (A) value was used to calculate percentage transparency (T) using the equation below  $A = 2 - \log_{10} \%T$

## **3.9. Biological characterization of oligomers and hydrogels**

### **3.9.1 Cytotoxicity**

In vitro cytocompatibility of OPF and APVA oligomers and its hydrogels were assessed with L929 fibroblast cells purchased from NCCS, Pune. The cells were cultured in complete DMEM containing high glucose supplemented with 10% fetal bovine, 1% antibiotic–antimycotic solution serum and 0.37% sodium bicarbonate. Cells were cultured at 37°C in a humidified 5% CO<sub>2</sub> incubator.

### **3.9.2. MTT Assay of oligomers**

OPF resin (300 mg/ml) and APVA resin (100 mg/ml) were diluted in PBS and was filtered through a 0.22 µm filter. A concentration range between 150 mg/ml - 2 mg/ml was prepared with DMEM medium and incubated at 37 °C for 24 h. Then, L929 cells were seeded onto a 96 well tissue-culture plate and incubated under CO<sub>2</sub> at 37 °C and cultured to

70% confluency. After 24 h, 100  $\mu$ l of the diluted polymer resin solutions were seeded on to the cells and incubated for 24 h in a CO<sub>2</sub> incubator. Each sample was taken in a triplicate. After 24 h incubation, the samples were aspirated and 40  $\mu$ l of MTT (5mg /PBS) solution was added and incubated for an additional 4 h at 37 °C. Then, 200  $\mu$ l of DMSO was added to dissolve the formazan crystals formed and the plate was kept for 30 min at RT. The absorbance at 570 nm was recorded using a UV/Vis microplate reader (Varian, Cary 50, and USA).

### ***3.9.3. Direct Contact Assay***

The OPF and APVA hydrogels were prepared under sterile conditions. The diluted polymer resins prepared in PBS with PEGDA crosslinker and both initiators, APS and TEMED, were filtered through a sterile 0.22  $\mu$ m filter. Hydrogels were prepared in a 48-well cell tissue culture plate and were incubated in 1.5 ml of DMEM medium for 72 h at 37°C. After 72 h, 10 mg weight of hydrogels were directly placed into the wells of a 24-well plate containing 80% confluent L929 fibroblast cell monolayers.. After 24 h incubation, pictures were taken using a fluorescent microscope (Olympus IX71). to evaluate the morphology of cells.

### ***3.9.4. Live /dead cell assay of direct contact***

Cells from direct contact method were incubated with PBS containing 5 mg of acridine orange and 5 mg of ethidium bromide for 5 min. Cells were again washed with PBS and images were taken using a fluorescent microscope(Olympus IX71).

### ***3.9.5. MTT Assay of Hydrogels***

OPF and APVA hydrogels were prepared under sterile conditions as described previously. The prepared hydrogels were incubated in 1.5 ml DMEM medium for 72 h at 37°C in a sterile 48-well tissue culture plate. The leachable containing medium was used as for cell viability test.

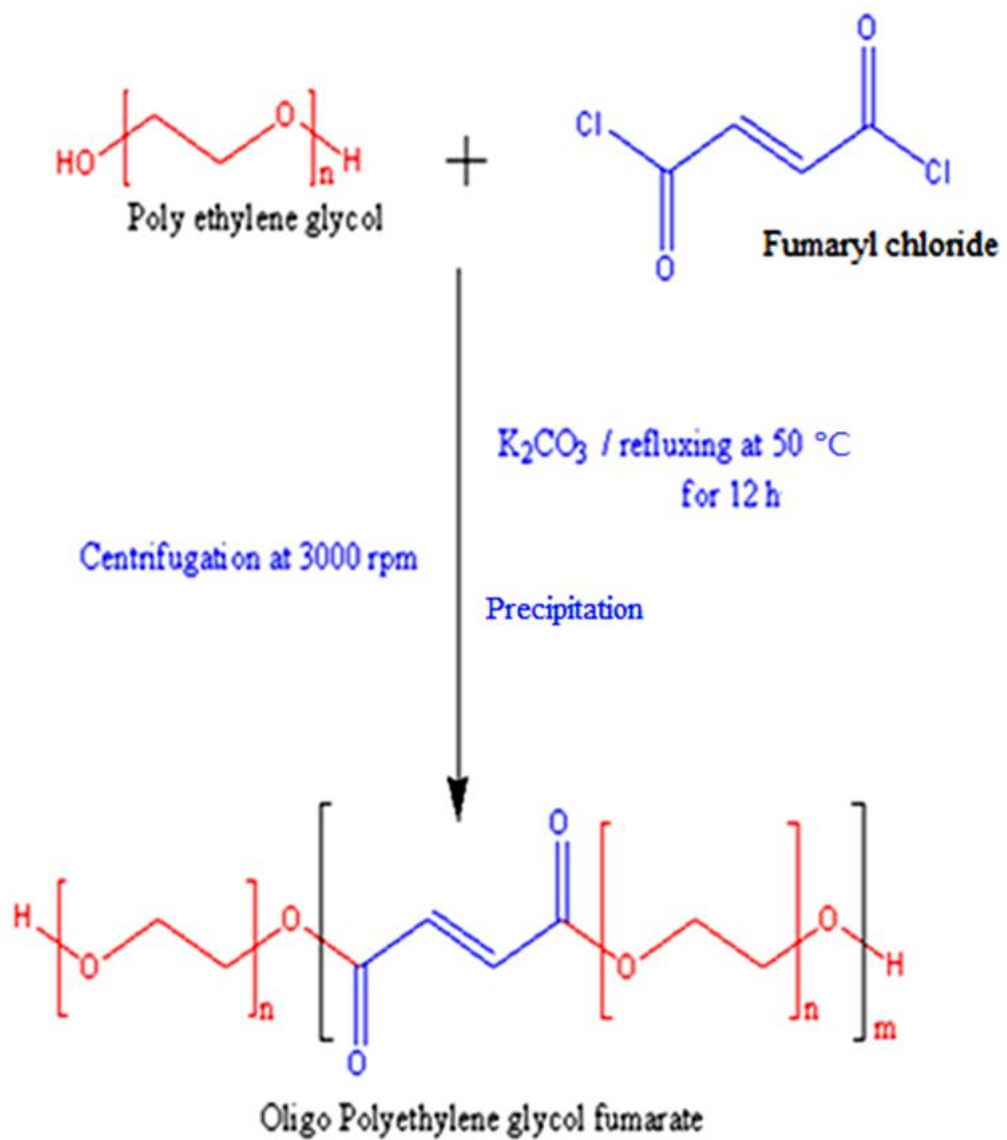
## Chapter IV

### RESULTS AND DISCUSSION

#### 4.1. Synthesis of oligomers and pregel formulations

##### *4.1.1. Polyethylene glycol fumarate oligomer (OPF)*

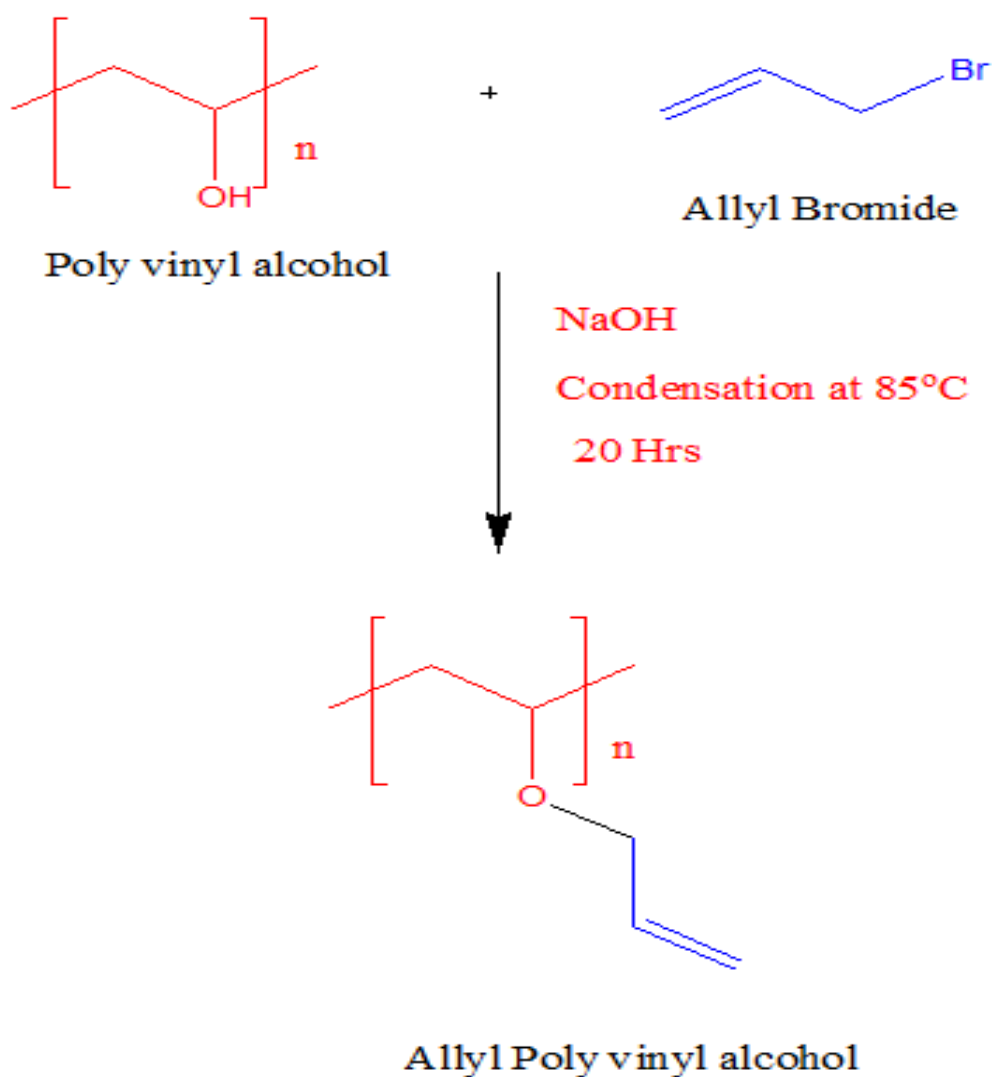
The schematic representation for the synthesized polyethylene glycol fumarate oligomer is shown in Scheme 4.1. The reaction of polyethylene glycol and fumaryl chloride has resulted in a light yellow coloured viscous liquid. This OPF liquid; a linear polyester, is formed via a condensation reaction in the presence of potassium carbonate as a proton scavenger. Proton scavengers such as  $K_2CO_3$  and triethylamine have been utilized in the synthesis of OPF.<sup>49</sup> However, the use of  $K_2CO_3$  results in a light colored product which is beneficial for the present application. OPF resin also has an added advantage of finite chain length of PEG block and fumarate double bond which offer fixed crosslinks in the formation of OPF hydrogels.<sup>51</sup>



**Scheme 4.1. Schematic representation of synthesis of oligo polyethylene glycol fumarate**

#### 4.1.2. Allyl - poly vinyl alcohol

The reaction scheme for the synthesis of allyl-poly vinyl alcohol is shown below (Scheme 4.2). The nucleophilic substitution reaction between polyvinyl alcohol and allyl bromide was conducted at 85 °C for 20 h in the presence of sodium hydroxide. A light yellow coloured liquid with a pungent HBr smell was obtained as product. The excess byproduct was removed by rotary evaporation and the product purified by dialysis to give a pale yellow colored solution. The final product was obtained after lyophilisation.



Scheme 4.2 .Schematic representation of synthesis of allyl-poly vinyl alcohol.

## 4.2. Characterization of pregel formulation

### 4.2.1. Spectral analysis of oligo polyethylene glycol

The chemical composition of the polyethylene glycol fumarate oligomer was confirmed using  $^1\text{H}$ NMR spectrum as depicted in figure 4.1.

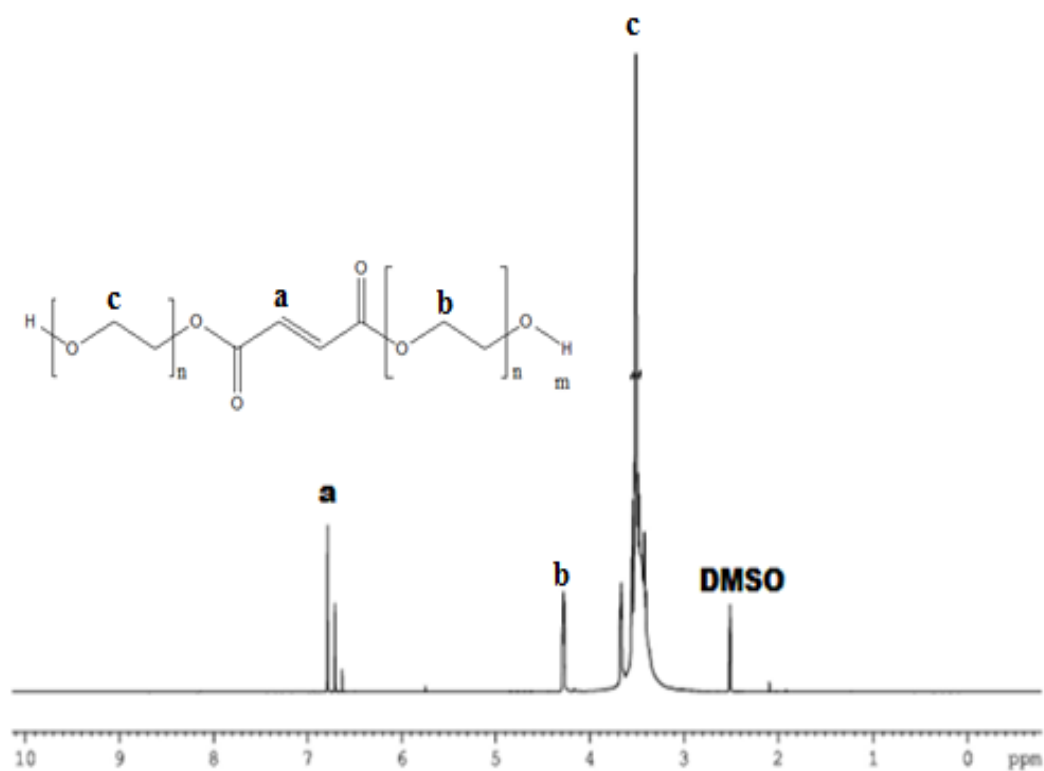


Fig.4.1.  $^1\text{H}$ -NMR spectrum of oligo polyethylene glycol fumarate

The spectrum displayed peaks at 6.78 ppm and 6.706 ppm confirming the presence of fumarate groups. The peaks at 3.40 - 4.29 ppm and 4.273 ppm correspond to the methylene groups in PEG and fumarate group adjacent to PEG respectively.

#### 4.2.2. Spectral analysis of allyl polyvinyl alcohol

The  $H^1$ NMR spectrum of allyl polyvinyl alcohol oligomer confirms the allyl group substitution in the polyvinyl alcohol (figure 4.2). The characteristic peaks in the region, 5.703-5.918 ppm, confirm the presence of allyl group. Similar substitution of allyl group was reported by Ming Kuo et al.<sup>52</sup> The multiple peaks around 3.801 - 3.897 ppm corresponds to the protons near the ether group.

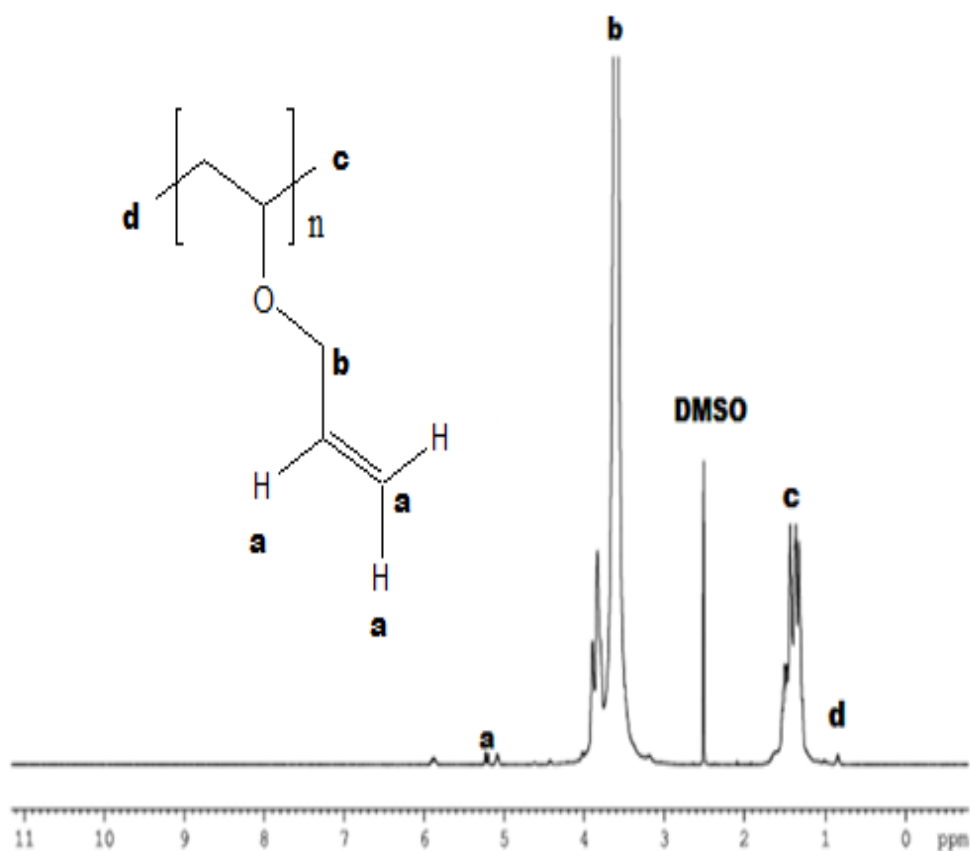


Figure.4.2.H-NMR spectra of allyl polyvinyl alcohol oligomer

### 4.2.3 FTIR analyses of oligo polyethylene glycol fumarate (OPF)

Fourier transform infrared spectrum of OPF oligomer is shown in figure 4.3. The characteristic stretching at  $2874\text{ cm}^{-1}$  and  $3425\text{ cm}^{-1}$  belong to  $-\text{CH}$  and  $-\text{OH}$  groups respectively. The spectrum further displays bands at  $1644\text{ cm}^{-1}$  and  $1455\text{ cm}^{-1}$  corresponding to  $\text{C}=\text{C}$  stretching and methylene asymmetric bending respectively.<sup>49</sup> The pertinent peak for ester unit was observed at  $1721\text{ cm}^{-1}$  and the presence of the poly(ethylene glycol) unit is confirmed with the appearance of  $-\text{C}-\text{O}-$  stretching of ether group at  $1180\text{ cm}^{-1}$ .<sup>51</sup>

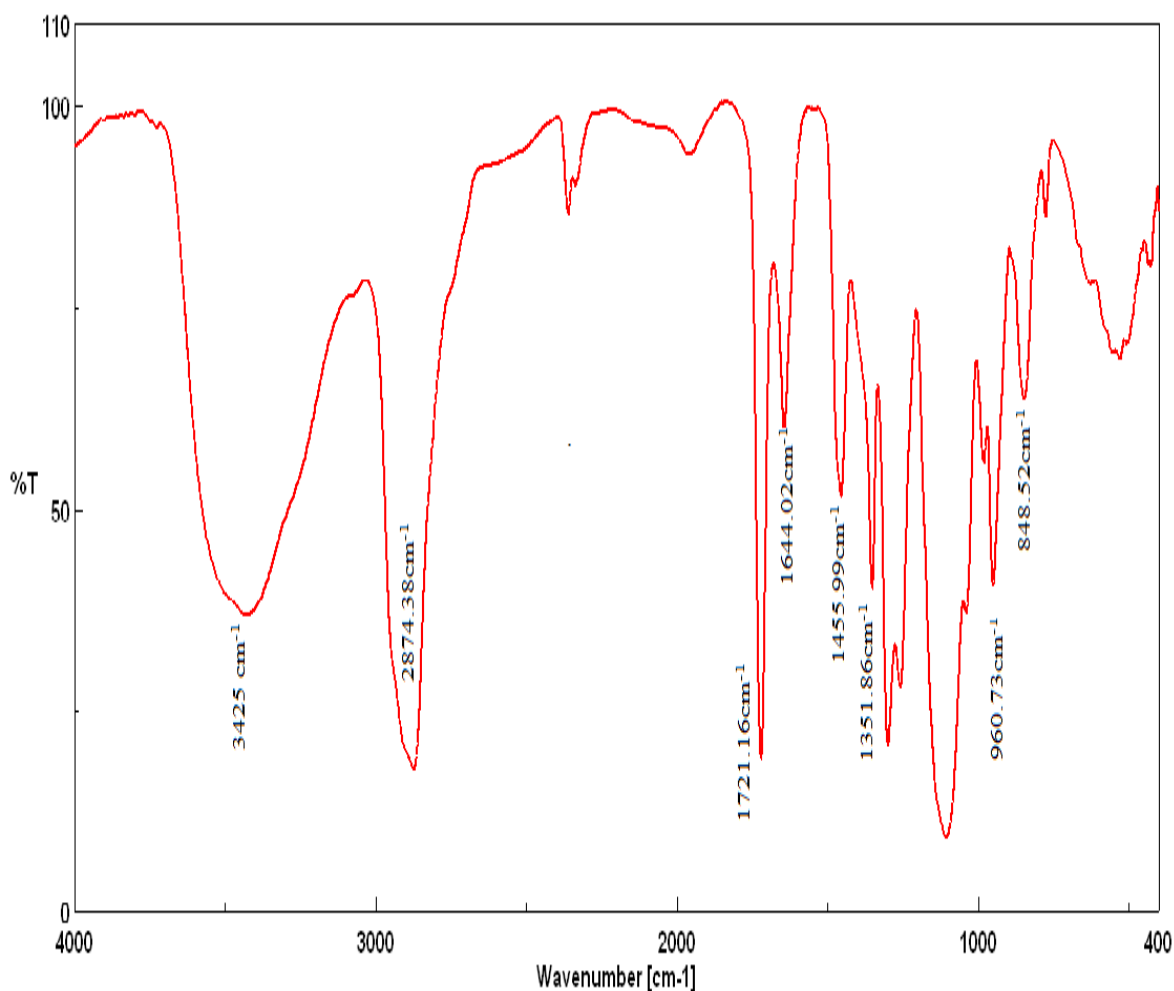


Figure 4.3 FTIR spectrum of oligo polyethylene glycol fumarate

#### 4.2.4. FTIR analysis of allyl poly vinyl alcohol oligomer

Fourier transform infrared spectrum of APVA oligomer is shown in figure.4.4. The peaks obtained in the spectrum confirm the successful conversion of PVA to allyl substituted PVA. The characteristic peaks at  $1655\text{ cm}^{-1}$  and  $1086\text{ cm}^{-1}$  correspond to C=C stretching of the double bond in allyl group and the ether bond in allyl PVA respectively.<sup>53</sup> The spectrum also displayed the characteristic broad band at  $3264\text{ cm}^{-1}$  corresponding to the OH group in PVA.

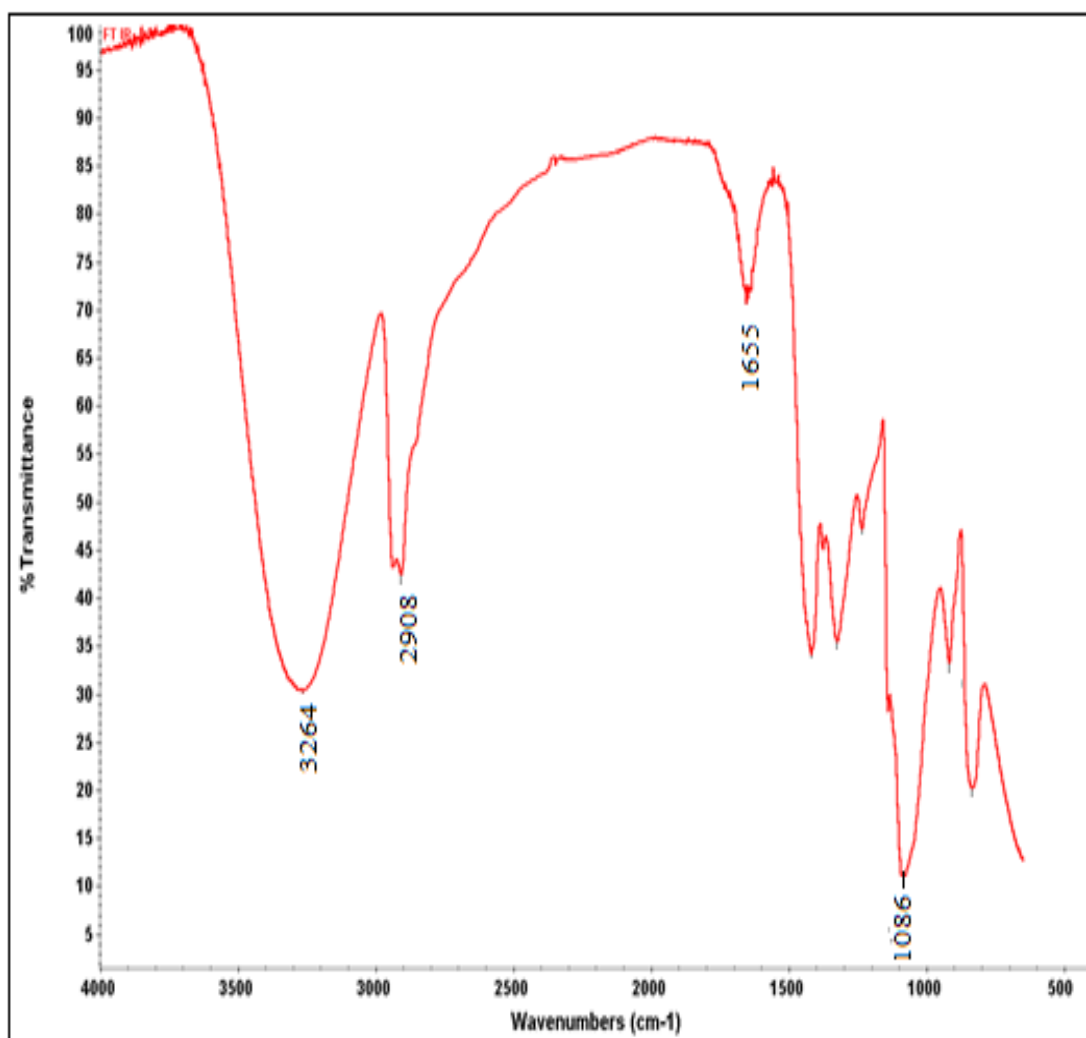


Figure 4.4. FTIR spectra of allyl poly vinyl alcohol oligomer

#### 4.2.5. GPC analysis of oligomers

The molecular weight of oligomers was determined using GPC. The synthesized OPF and APVA oligomers molecular weight values are given in Table 4.1. It showed weight average molecular weight of 7438 with poly dispersity of 1.30 confirming oligomer formation. The substitution of allyl group in the polyvinyl alcohol gives the number average molecular weight of 11484 with poly dispersity of 2.91.

**Table 4.1. Molecular weight data of oligomers**

<b>Pregel resin</b>	<b>Mn</b>	<b>Mw</b>	<b>MP</b>	<b>Poly dispersity</b>
Oligo PEG fumarate	5742	7438	6911	1.30
Allyl PVA	3949	11484	5791	2.91

#### 4.2.4. Viscosity of pregel formulations

The studies on viscosity of pregel formulations determined using a rotational viscometer reveal viscosity in the range of 30-32 cp and 30-34 cp for pregel formulations of OPF and APVA oligomers respectively.

### 4.3. Preparation of Hydrogels

#### 4.3.1. OPF based hydrogels

OPF based hydrogels possess low protein absorption properties, minimal inflammatory effect and good safety for *in vivo* uses. OPF hydrogels were prepared from the synthesized OPF resin via free radical initiation with PEGDA crosslinker as shown in (Table 4.2). In general, crosslinking of injectable hydrogels are initiated by physical interaction between polymer chains or via chemical crosslinking such as disulphide bond formation, Michael addition reaction etc. Compared to physical crosslinking, chemical crosslinking gives improved mechanical properties and tunable degradation profiles. In this experiment the OPF hydrogels were prepared using APS and TEMED as initiators. Crosslinking of the hydrogels are initiated between the double bonds of fumarate groups present in the OPF chains. Different concentrations of PEGDA crosslinker were used for varying hydrogel characteristics (Table 4.2).

**Table 4.2 OPF hydrogel formulations and setting characteristics**

<b>Hydrogels</b>	<b>OPF (30%solution)</b>	<b>PEGDA</b>	<b>APS</b>	<b>TEMED</b>	<b>Setting time (min)</b>	<b>Setting Temperature (°C)</b>
OPFI	400 $\mu$ L	6 mg	24 $\mu$ L	8 $\mu$ L	21	32
OPFII	400 $\mu$ L	12 mg	24 $\mu$ L	8 $\mu$ L	8	32
OPFIII	400 $\mu$ L	16 mg	24 $\mu$ L	8 $\mu$ L	4	32

The representative image of the prepared OPF hydrogels with APS and TEMED as initiators is shown in Figure. 4.5. The different percentage crosslinker incorporated hydrogels showed different setting time at RT. It was observed that the setting time showed an inverse relationship to the percentage of crosslinker used. The non-polarized double bond of the fumarate ester group in OPF is far less reactive than acrylic ester and hence do not undergo easily self-crosslinking. Hence, crosslinker molecules are typically added to initiate crosslinking and reduce crosslinking time.<sup>54</sup> The schematic representation of crosslinking and formation of hydrogel is shown in the Scheme 4.3.

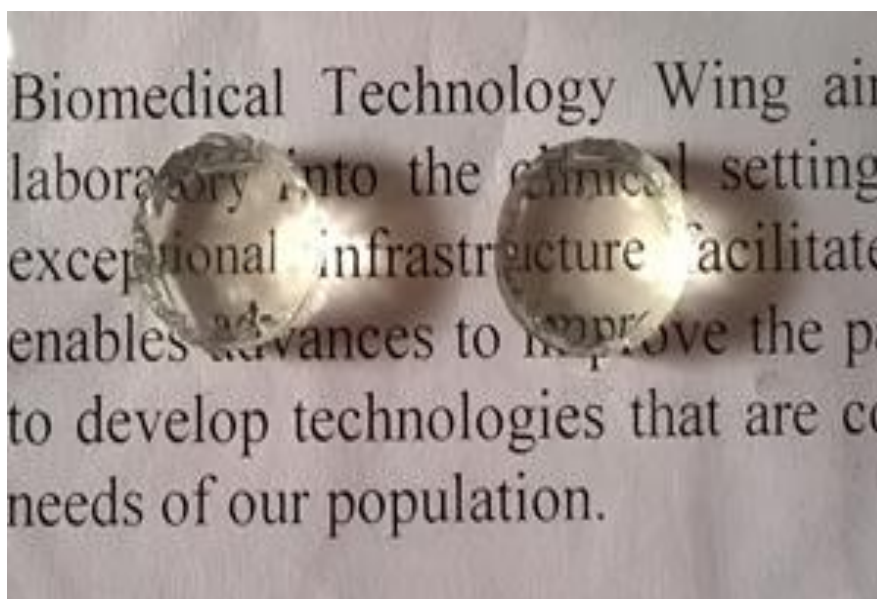
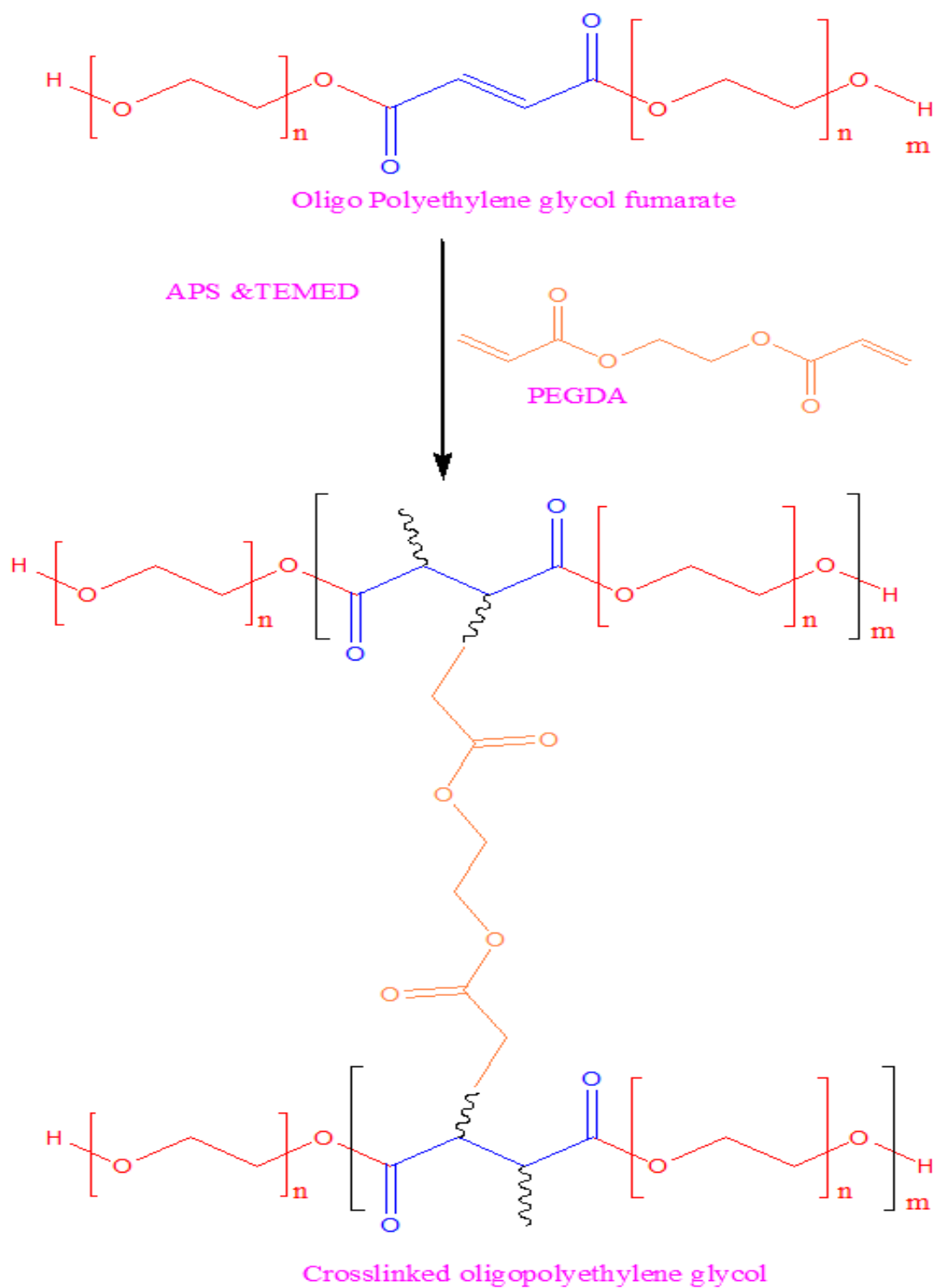


**Figure 4.5. Prepared OPF hydrogels**



**Scheme 4.3 Crosslinking of OPF oligomer in the formation of hydrogel**

#### 4.3.2. APVA based hydrogels

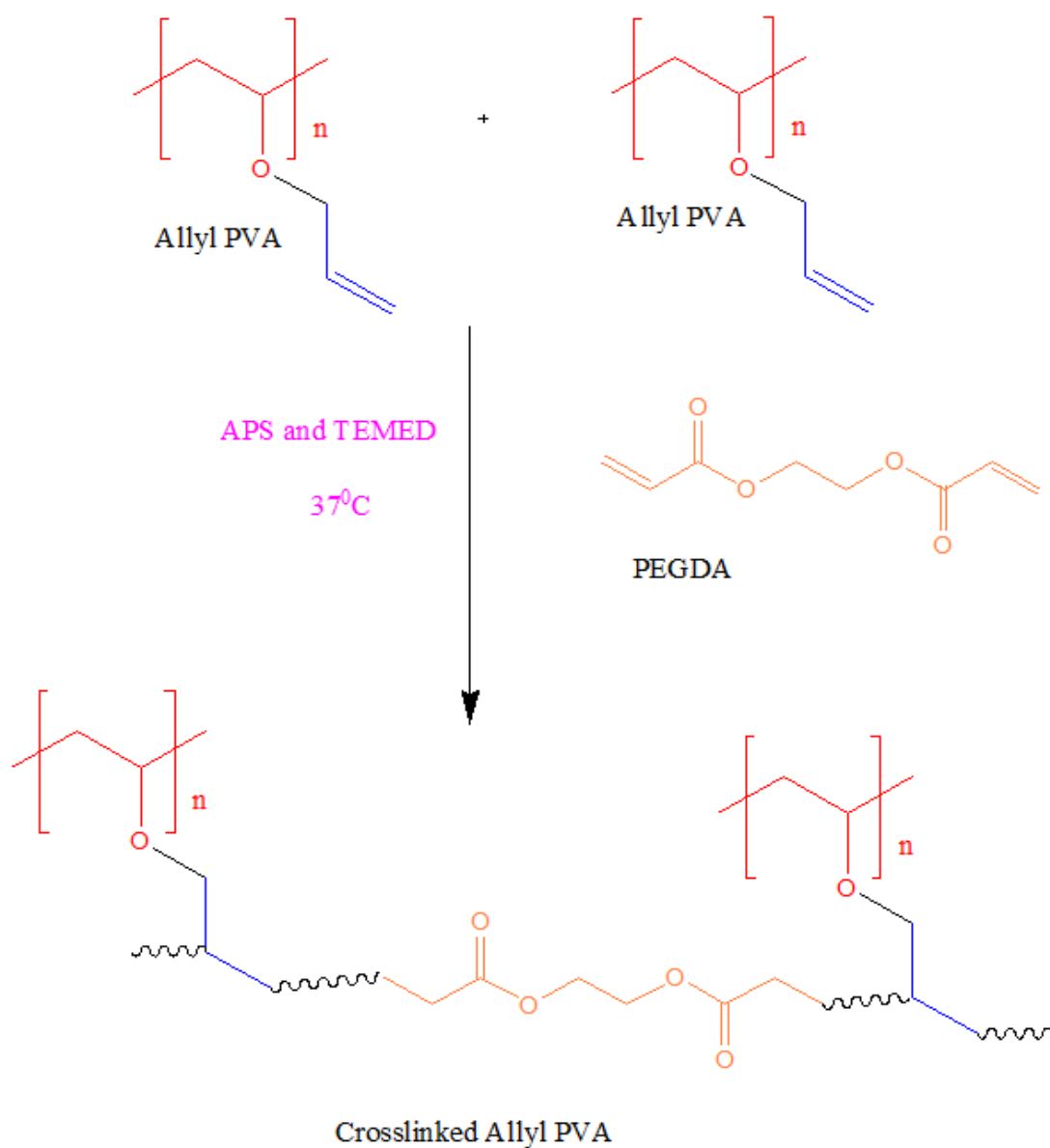
Poly vinyl alcohol based hydrogel have so many ocular applications because of its excellent transparency property. Allyl-poly vinyl alcohol.oligomer based hydrogel hydrogels were prepared using APVA resin by free radical polymerization with different percentage PEGDA crosslinker (Table 4.3). The hydrogel setting time varies with different percentage of crosslinker used. APVA hydrogels prepared with different percentage crosslinker are represented as APVAI, APVAII, and APVAIII (Table 4.3). The experimental data revealed that the setting time showed an inverse relationship with the percentage of crosslinker used.

**Table 4.3. APVA hydrogel formulations and their setting characteristics**

<b>Hydrogel</b>	<b>Allyl PVA (10% Solution)</b>	<b>PEGDA</b>	<b>APS</b>	<b>TEMED</b>	<b>Setting time (min)</b>	<b>Setting Temperature (°C)</b>
APVAI	400 µL	10 mg	24 µL	8 µL	3	32
APVAII	400 Ml	12 mg	24 µL	8 µL	2	32
APVAIII	400 Ml	16 mg	24 µL	8 µL	1	32

Chemical crosslinking gives good strength and desired gel strength. Hence APVA hydrogels were prepared using 10% allyl PVA oligomer with different percentage of PEGDA crosslinker (10%, 12%, 16%). APS and TEMED were used as initiators for gel crosslinking and the hydrogels were prepared in 48 well cell culture plate. The schematic

representation of cross-linked APVA hydrogel is shown in Scheme 4.4. The formed hydrogels were showed in the Figure 4.6.



**Scheme 4.4 Crosslinking of APVA oligomer in the formation of hydrogel**

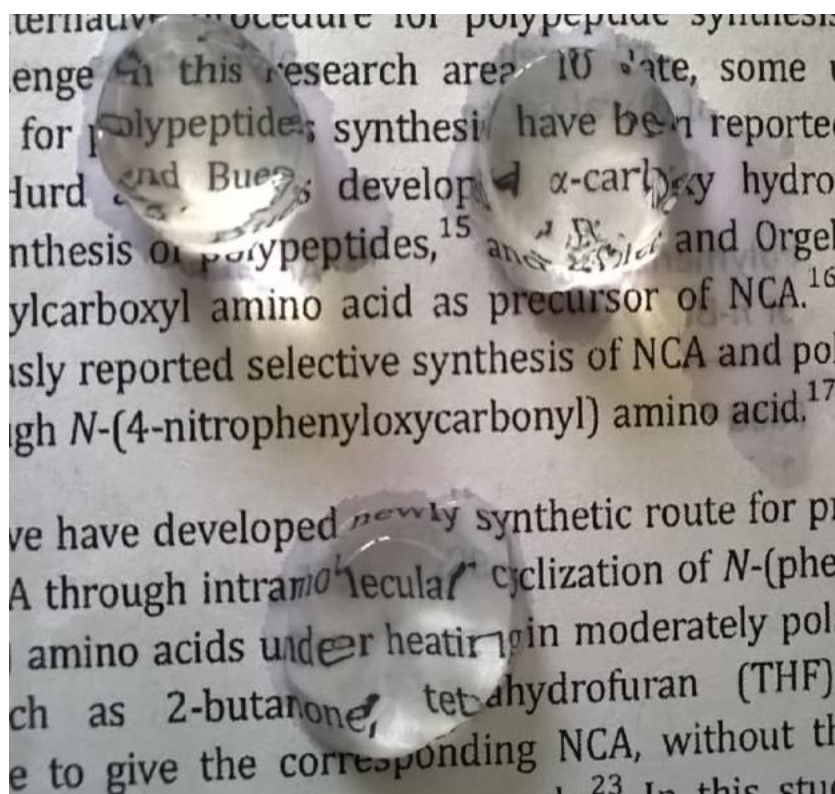


**Figure 4.6. Prepared APVA hydrogels**

#### **4.4 Hydrogel physiochemical properties**

##### ***4.4.1. Swelling studies of OPF hydrogels***

The weight swelling ratio and equilibrium water content of the prepared OPF hydrogels with different crosslinker concentrations are given in Figure 4.7. The data reveal increased swelling in water than in PBS. The equilibrium water content (EWC) of OPFI, OPFII, OPFIII hydrogels in PBS are 73.62, 70.80, 68.36 whereas in water they are 76.39, 73.21., 74.06 respectively. It was observed that swelling ratio and EWC of hydrogels decreased with increasing crosslinker concentration.

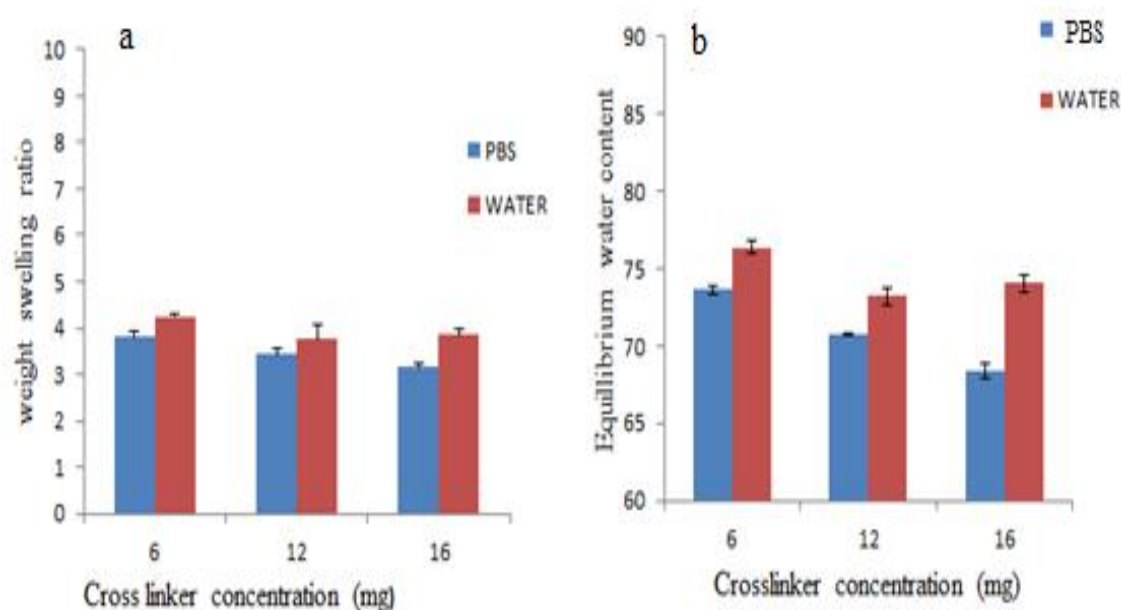


**Figure 4.7. (a) Weight swelling ratio and (b) Equilibrium water content of the OPF hydrogels (Data represents mean+SD with n=4 samples)**

#### **4.4.2. Swelling studies of APVA hydrogels**

The weight swelling ratio and equilibrium water content of the formed APV hydrogels with different crosslinker concentrations are given in Figure 4.8. The swelling ratio and EWC of hydrogels showed increased swelling in water than PBS. The equilibrium water content of APVAI, APVAII, APVAIII hydrogels in PBS were 86.12, 84.69, 82.39 whereas in water it was observed to be 85.72, 84.52, 81.71 respectively. Again, as crosslinker concentration increased, the swelling ratios and EWC decreased gradually. When compared to OPF hydrogels, APVA hydrogels have better water swelling capacity which is desired for the development of artificial VS.

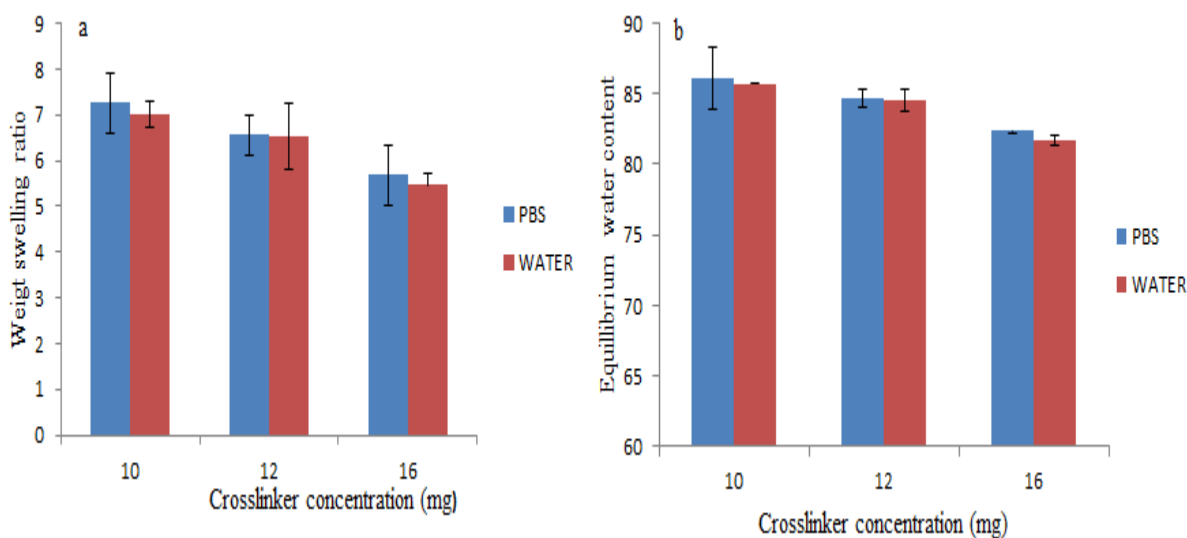


**Figure 4.8. (a) Weight swelling ratio and (b) Equilibrium water content of the prepared APVA hydrogels**

#### ***4.4.3 Crosslink density and molecular weight between crosslinks of hydrogels***

The crosslink density and molecular weight between crosslinks depicts the physiochemical properties of hydrogels. The crosslink density of OPF and APVA hydrogels in water are shown in Table 4.4. In general, crosslinked hydrogels with higher crosslink density absorb less water in compared to hydrogels with lesser crosslink density.<sup>55</sup> The crosslink density increases with increasing crosslinker concentration. Also, molecular weight between crosslinks decreases with increasing crosslink density. Compared to OPF hydrogels, APVA hydrogels have less crosslink density and hence more molecular weight between the crosslinks. Furthermore, the swelling property of the hydrogel increases with decreased crosslinking density. In the case of APVA hydrogels, the hydrogels were prepared with 10% APVA pregel solution whereas OPF hydrogels were obtained from 30% OPF polymer solution. This explains the increase in water uptake capacity of APVA hydrogels which have lower crosslink density compared to OPF hydrogels. It is also

reported that with low PVA content in Salcan/PVA hydrogels, the physical crosslink density decreased leading to increased swelling properties.<sup>56</sup>

**Table.4.4. Crosslink density and molecular weight between crosslinks of hydrogels**

<b>Hydrogels</b>	<b>Crosslink density (<math>\times 10^{-3}</math> mol cm<sup>-3</sup>)</b>	<b>Molecular weight between crosslinks (g cm<sup>-3</sup>)</b>
OPFI	17.097	58.48979
OPFII	17.497	57.15265
OPFII	18.829	53.10888
APVAI	14.323	69.81736
APVAII	14.491	69.00767
APVAIII	15.832	63.16125

#### **4.4.4. Mechanical Property**

The influence of crosslinker concentration on the mechanical properties of hydrogels was investigated. As shown in Table 4.5, both OPF and APVA hydrogels showed an increasing trend in mechanical properties with increasing crosslinker concentration. APVAI hydrogels were too soft and did not maintain their shape for evaluating mechanical properties because of their high water content. The OPFI, OPFII, OPFIII showed a compressive strength of 41.748 kPa, 59.85 kPa, and 72.97 kPa while APVAII and APVAIII showed compressive strength of 0.538 kPa and 1.025 kPa respectively.

**Table 4.5. Mechanical properties of OPF and APVA hydrogels**

<b>Hydrogels</b>	<b>Maximum load at break (N)</b>	<b>Young modulus (kPa)</b>	<b>Compressive strength (kPa)</b>
<b>Oligo polyethylene glycol fumarate based hydrogel</b>			
OPFI	3.433308	218.098	41.748
OPFII	2.40865	318.43	59.85
OPFIII	5.693393	392.14	72.97
<b>Allyl polyvinyl alcohol oligomer based hydrogel</b>			
APVAI	-	-	-
APVII	0.08008	5.028	0.538
APVIII	0.142058	6.803	1.025

#### **4.4.5. Degradation Studies**

Degradation studies of OPFII hydrogels were carried out in PBS solution. OPFII hydrogel having the optimized 12% crosslinker were selected for degradation studies. For degradation studies, the percentage of mass loss and pH changes were noted every 7 days for a period of 6 weeks as shown in Figure 4.9a. It was observed that 47% hydrogel degradation occurred in the first week following which degradation a constant. At the end of the 6<sup>th</sup> week, a total of 63 % degradation was observed in OPFII hydrogels. This is not surprising as OPF oligomers, composed of PEG-fumaric units, undergo ester hydrolysis and breakdown into their constituent parts.<sup>54</sup> OPFII hydrogels maintained neutral pH throughout the 6 week time period.

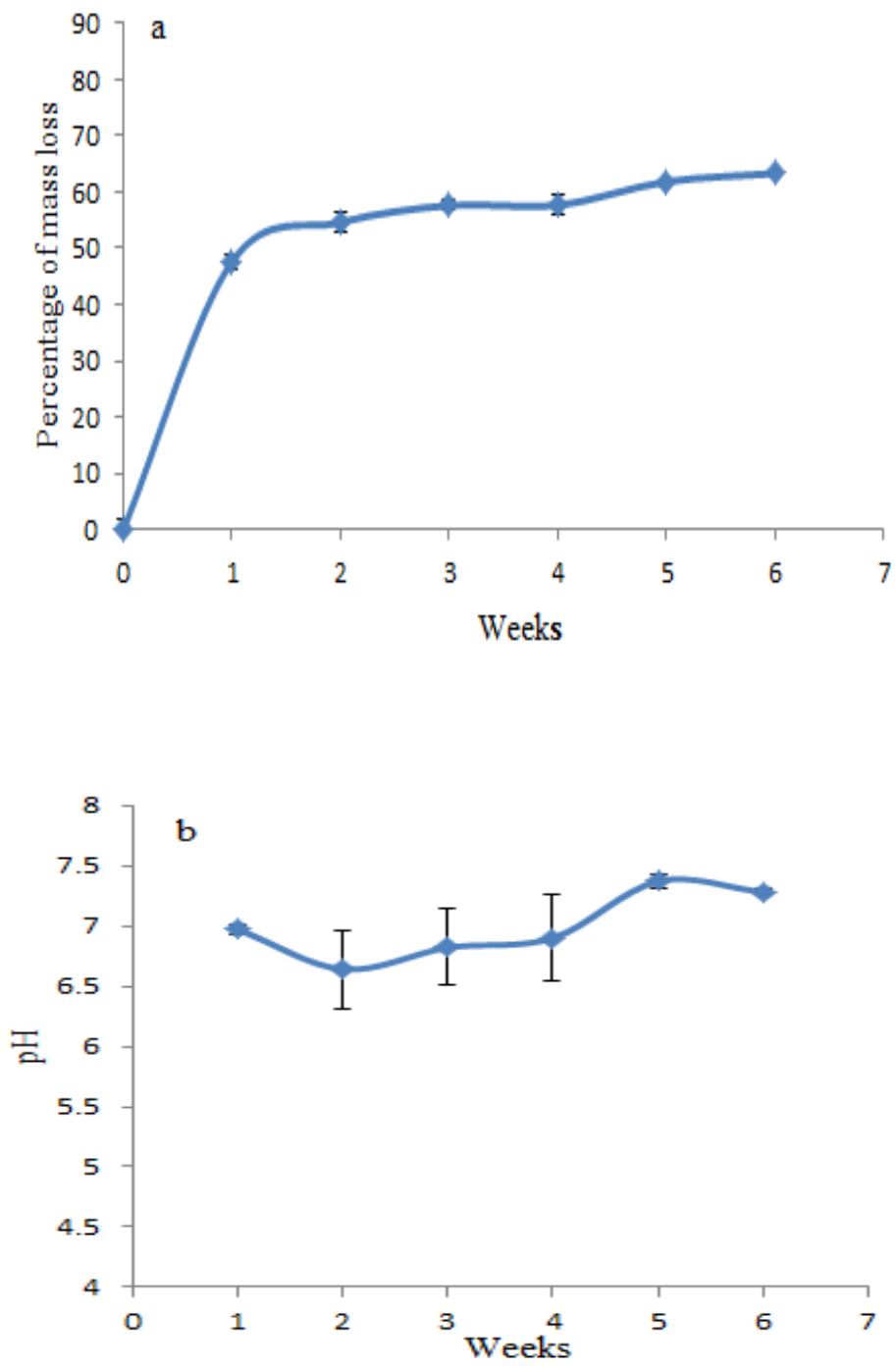


**Figure 4.9. Variation of mass (a) and pH (b) of the OPFII hydrogels during aging**

*APVA hydrogels*

In vitro degradation studies of APVAII hydrogels were performed for 6 weeks in PBS solution. The percentage weight loss and change in pH during the 6-week degradation period is shown in Figure 4.10.

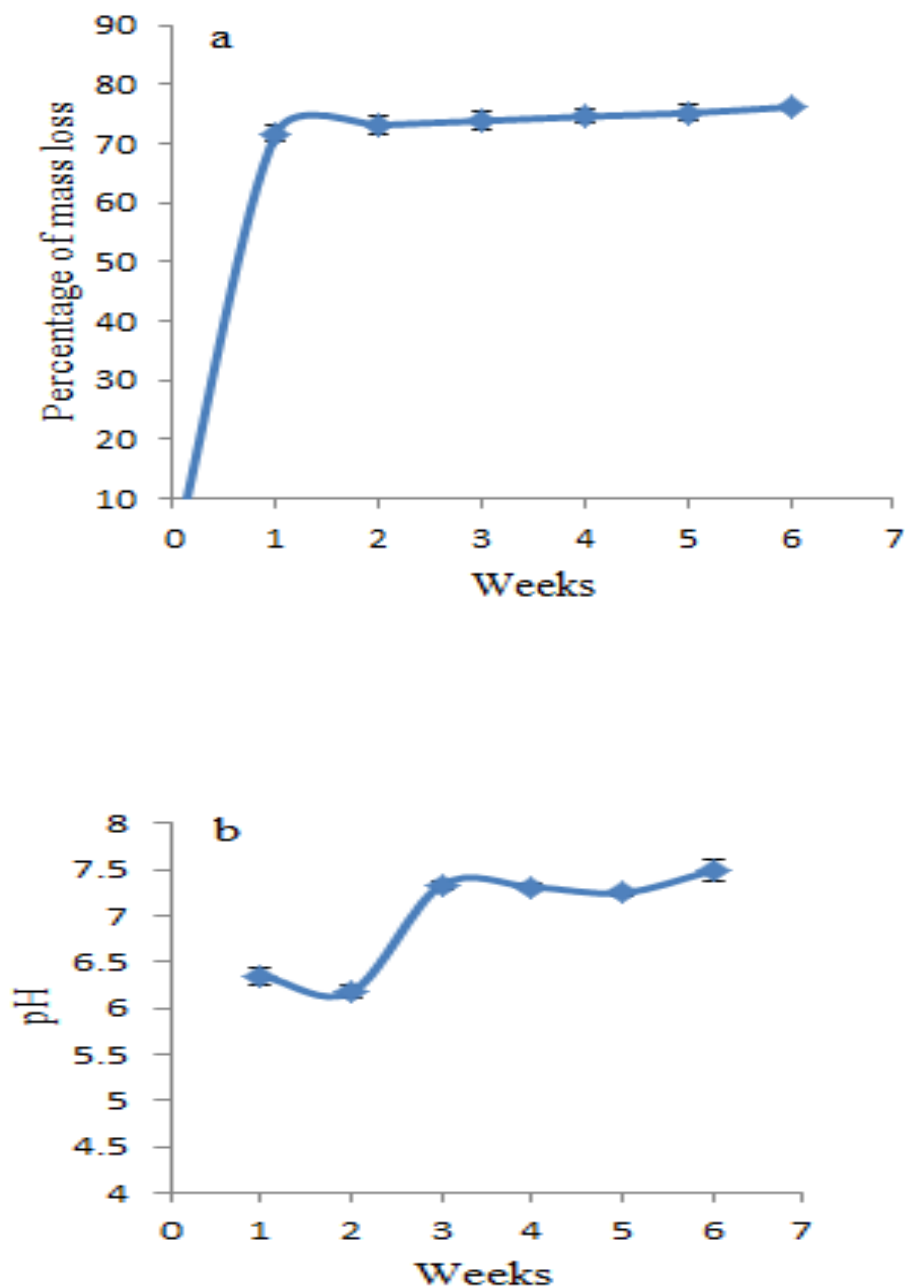


**Figure 4.10.** Variation of mass (a) and pH (b) of the APVAII hydrogels during aging

The pH variation during the degradation period was around neutral pH ranging between pH 6.3 to 7.8. Degradation profiles of APVAII hydrogels revealed 70% weight loss during the first week following which the rate remained constant until the end of the 6<sup>th</sup> week.

#### ***4.4.6. Surface Morphology***

##### *OPFII hydrogels*

The surface morphology of virgin and degraded OPFII hydrogels in PBS are shown in Figure 4.11. The SEM morphology of cross-sectioned fresh OPFII hydrogels showed a surface devoid of pores and cracks. After 3<sup>rd</sup> week, the hydrogel showed cracks and interconnecting pores because of degradation. Furthermore, pore size increased by the end of the 6<sup>th</sup> week.

##### *APVAII hydrogels*

The surface morphology of freshly prepared and degraded APVAII hydrogels are shown in Figure 4.12. As seen in the figure, the cross-sectioned surface of fresh APVAII hydrogels was devoid of pores and cracks. At 3<sup>rd</sup> and 6<sup>th</sup> week of degradation, a number of interconnecting pores were observed and appeared to increase gradually during the 6 week degradation study.

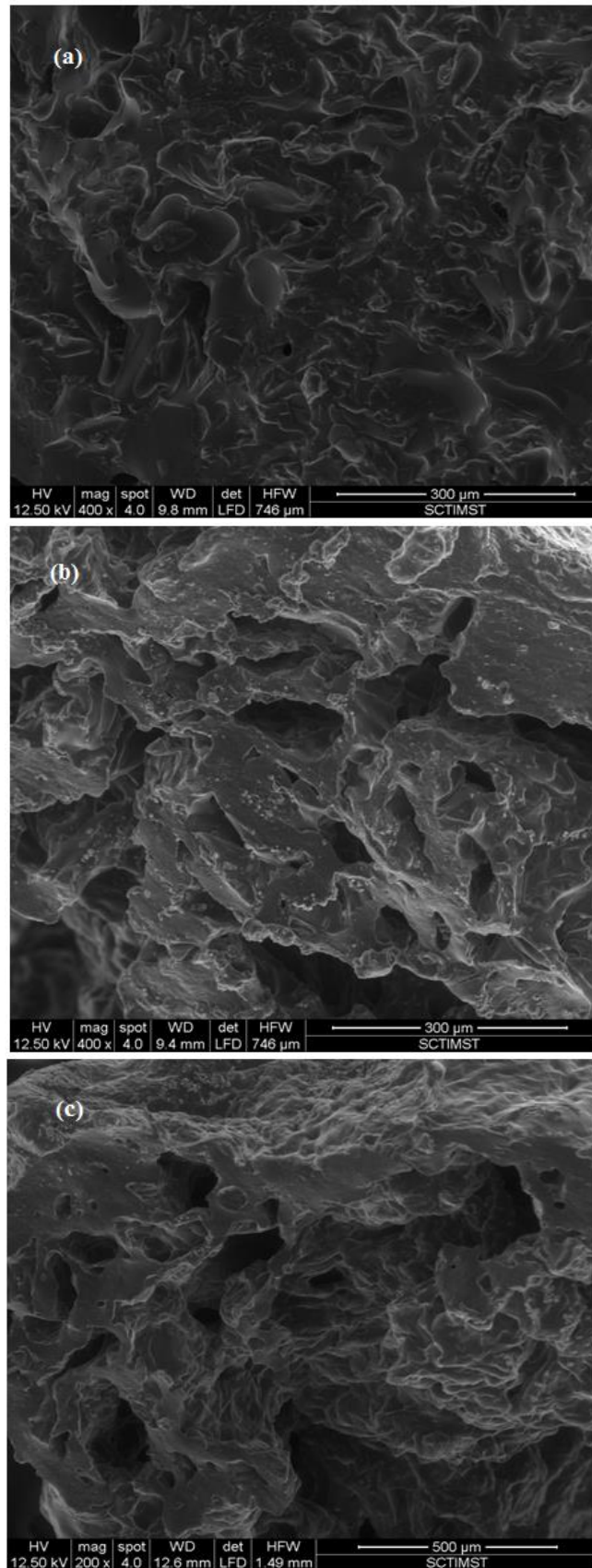


**Figure 4.11. Surface morphology of OPFII hydrogels. virgin hydrogel (a), hydrogel after 3<sup>rd</sup> week of aging (b) and hydrogel after 6<sup>th</sup> week of aging (c)**

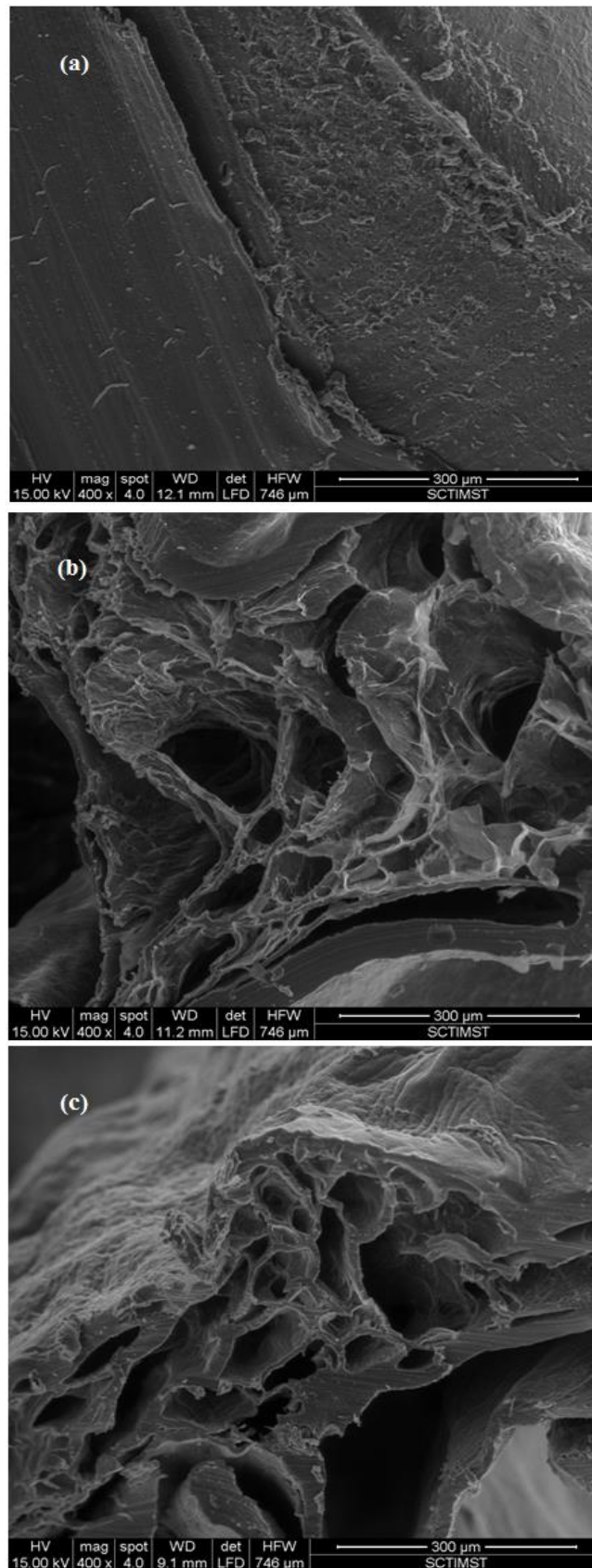


**Figure 4.12. Surface morphology of APVAII hydrogels. virgin hydrogel (a), hydrogel after 3<sup>rd</sup> week of aging (b) and hydrogel after 6<sup>th</sup> week of aging (c)**

## 4.5 .Thermal properties of hydrogel

### 4.5.1.DSC analysis of hydrogels

The property of water in hydrogels was analyzed by thermal analysis. The DSC curves of the OPFII and APVAII hydrogels are shown in Figure 4.13.

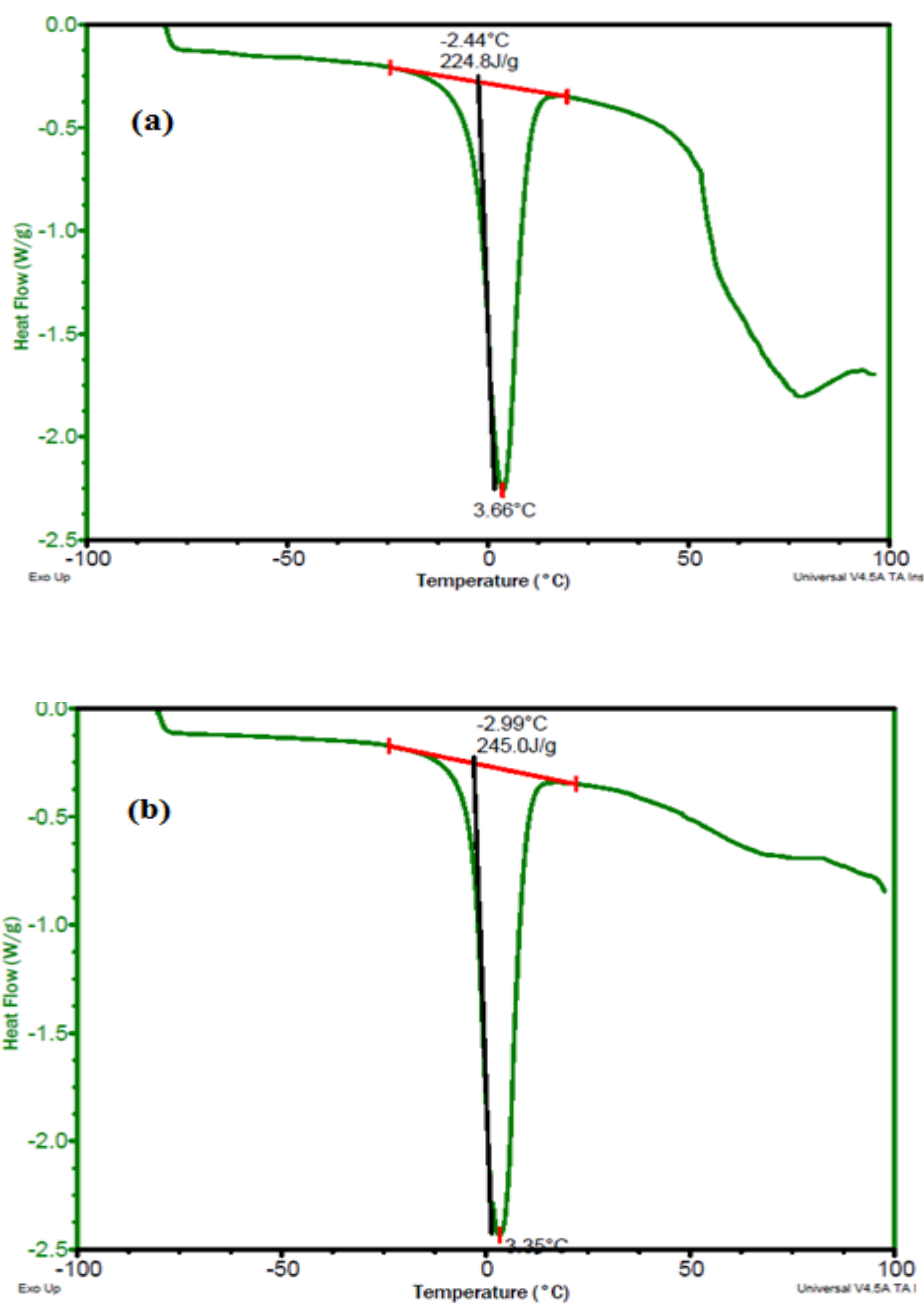


Figure 4.13. DSC curve of prepared hydrogels. (a) OPFII and (b) APVAII.

In the polymer network, water exists in more than two states, bound water and unbound water. The water molecules absorbed in the hydrophilic region are present in three forms, non-freezable bound water, freezable bound water, and free water. The non-freezable bound water is tightly hydrogen bonded water with undetectable phase transition. Freezable bound water interact weakly with the hydrogel molecule whereas free water does not interact in hydrogen bonding and hence both are categorized as freezable water.<sup>57</sup> In OPFII hydrogels, freezable water content was 67.305 % whereas non freezable water content was 5.95% (Table 4.6). In the case of APVAII hydrogels, freezable water content was 73.35% and non-freezable water content was 11.34%. The low free water content indicates good hydrophilic characteristics of the prepared hydrogels.

**Table 4.6. DSC analysis of hydrogels**

<b>Properties</b>	<b>OPFII</b>	<b>APVAII</b>
Enthalpy of melting of freezing water (J/g)	224.8	245
On set of crystallization of freezing water (°C)	-2.44	-2.99
Equilibrium water content(%)	73.21	85.42
Freezable free water content (%)	67.305	73.35
Non-freezable water content (%)	5.95	11.34

#### ***4.5.2.TG analysis of hydrogels***

TG curve of OPFII hydrogel is given in Figure 4.14. The curve; shows a two stage decomposition with significant mass losses obtained at 130 °C and 342 °C respectively. The decomposition temperature of OPFII was around 429 °C, as obtained in OPF/sodium methacrylate hydrogel systems<sup>58</sup>.

Sample: OPF  
Size: 7.3690 mg  
Method: UPTO 900

Directory: F:\sdtsc\TGA\2016  
Operator: TA  
Instrument: SDT Q600 V8.3 Build 101

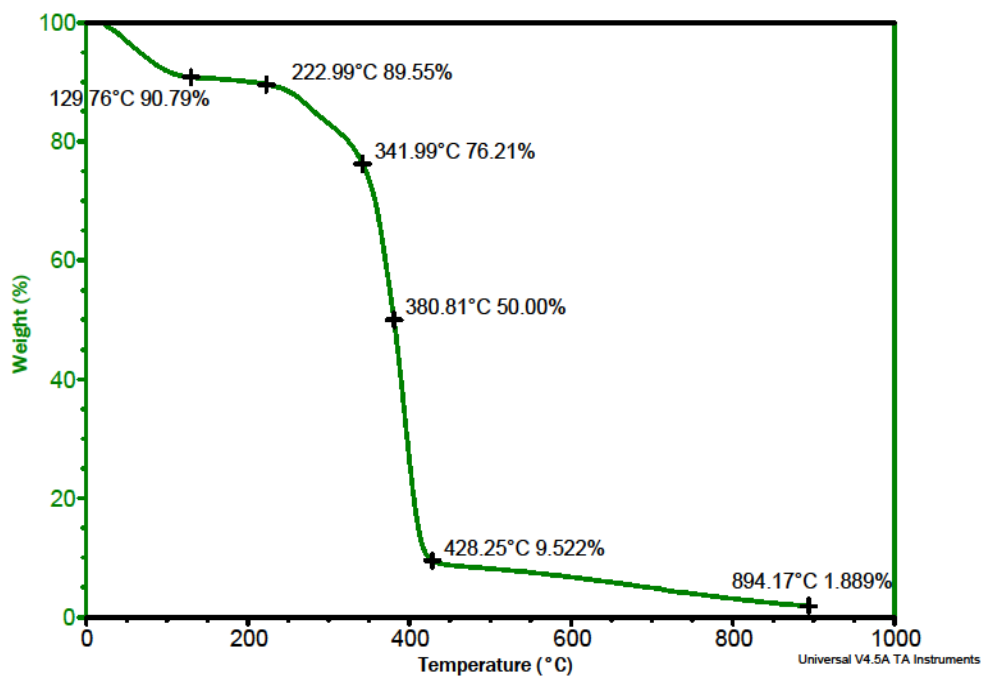


**Figure 4.14. TG curve of OPFII hydrogel.**

TG curve of APVAII hydrogel is given in Figure 4.15. The curve exhibits three zones of mass loss, corresponding to the degradation of the polymer components in accordance with reported literature<sup>59</sup> After the water loss step, the decomposition occurred mainly in the second degradation step that starts at 300 °C where it loses about 65 % of its mass and reflects the decomposition of side APVA chain. The second smaller step at 469 °C is attributed to the PVA main chain degradation. At 895 °C a residue of about 7.4% of the starting mass can be observed.

Sample: APV  
Size: 7.3000 mg  
Method: UPTO 900

Directory: F:\sdtsc\TGA\2016  
Operator: TA  
Instrument: SDT Q600 V8.3 Build 101

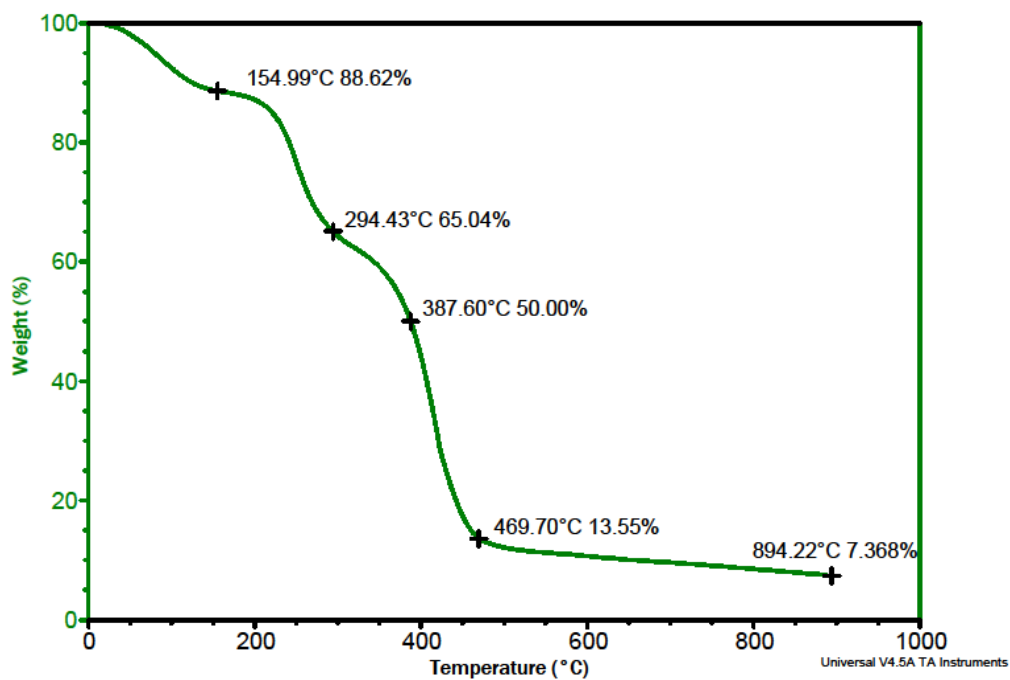


**Figure 4.15. TG curve of APVAII hydrogel.**

#### 4.6. Contact Angle Measurements

The contact angle measurements of OPF and APVA hydrogels are shown in in Figure 4.16. OPF hydrogel had a contact angle of  $58.90^\circ$  whereas APVA hydrogel exhibited a contact angle of  $65.5^\circ$ , both less than  $90^\circ$  indicating that the surface wetting characteristics are hydrophilic in nature.

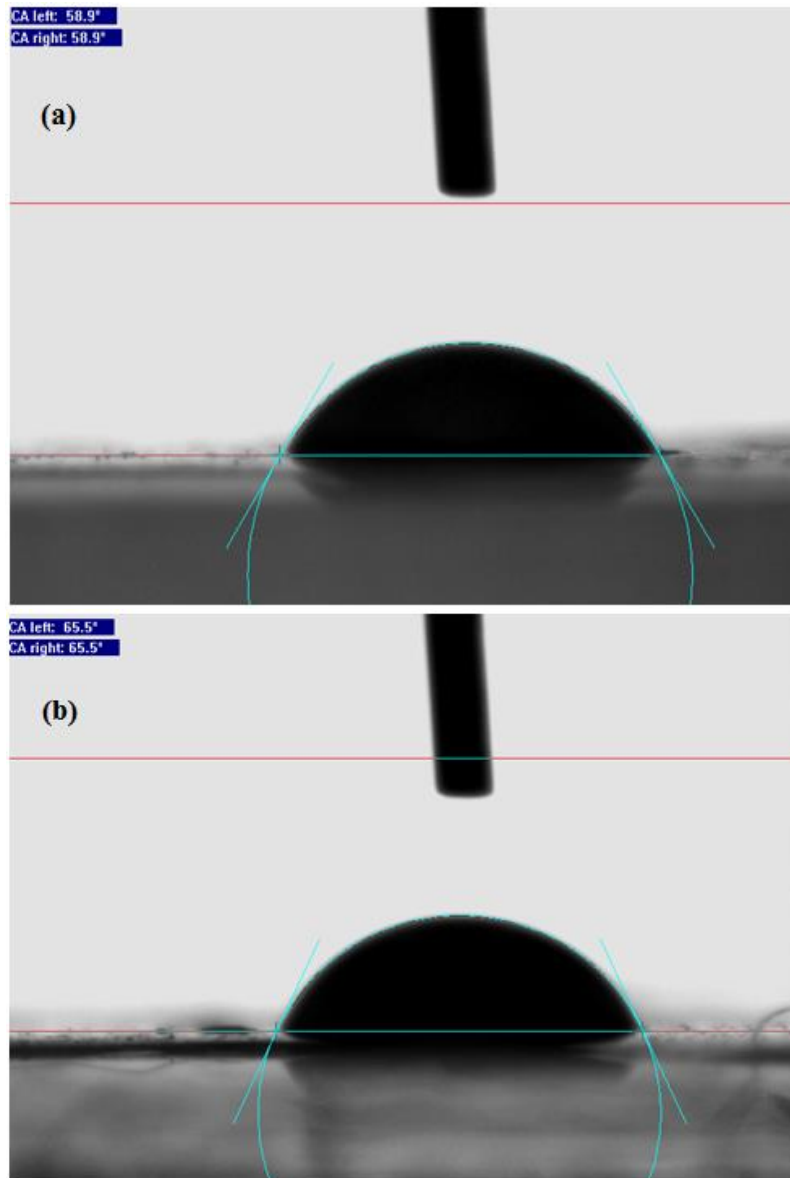


**Figure 4.16. Contact angle measurements.  
OPFII hydrogel (a) and APVAII hydrogel (b)**

#### ***4.7. Optical properties***

##### ***4.7.1. Refractive Index***

The refractive index value of OPFII and APVAII hydrogels are shown in Table 4.7. The refractive index of both hydrogels are in line with that of the native human vitreous

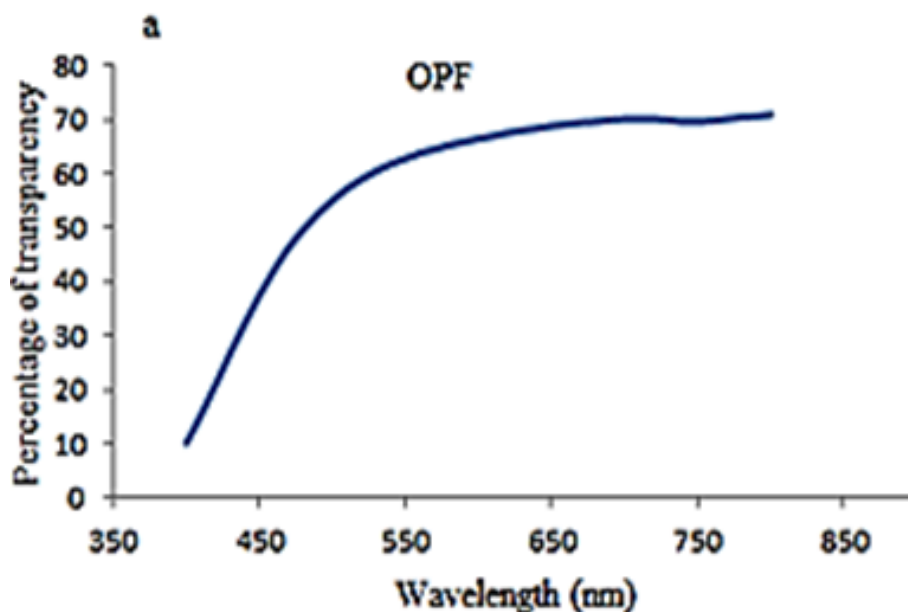
which is reported to range between 1.3345–1.3348.<sup>60</sup> Furthermore, a foldable capsular vitreous body (FCVB) injected with 3% PVA hydrogels showed a refractive index value of 1.3361.<sup>44</sup>

**Table 4.7. Refractive index of OPF and APVA hydrogels**

Hydrogels	Refractive index
OPFII	1.34060
APVAII	1.33232

*4.7.2. Transmittance*

The transparency of the vitreous substitute is important to mimic the optical characteristics of native vitreous. The transparency of OPFII and APVAII hydrogels in the range between 400 - 800 nm is shown in Figure 4.17. OPFII hydrogels exhibited 15.12 - 70.46% of transmittance whereas APVAII hydrogels showed 44.66 - 74.30% of transmittance in the measured range. PVA has been reported to have good optical properties and long term biocompatibility and could serve as a long-term artificial vitreous tamponade agent.<sup>60</sup>



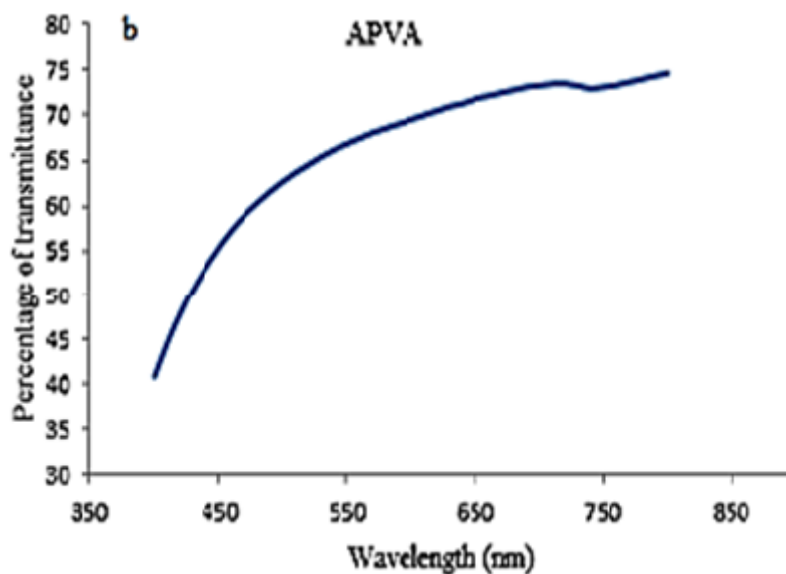
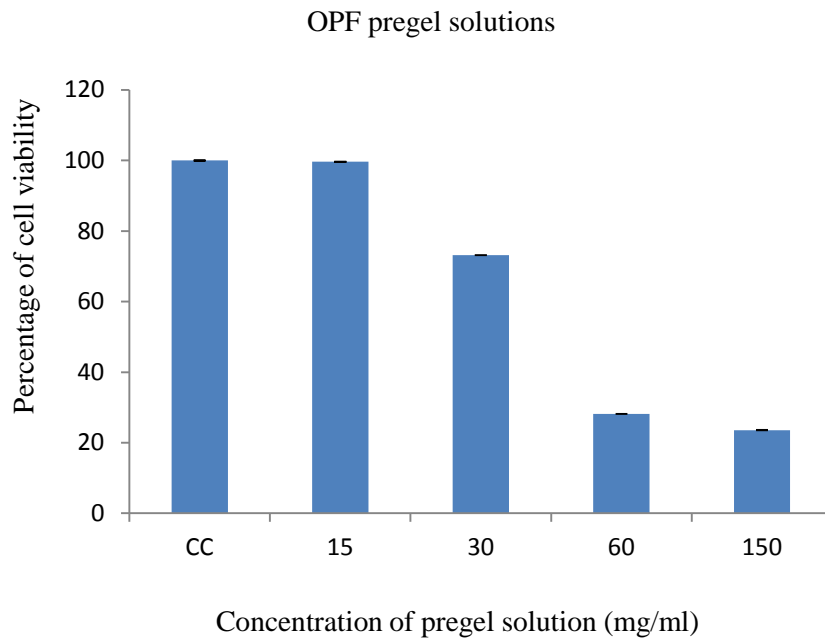


**Figure 4.17. Transparency of hydrogels. OPFII (a) and APVAII hydrogel (b)**

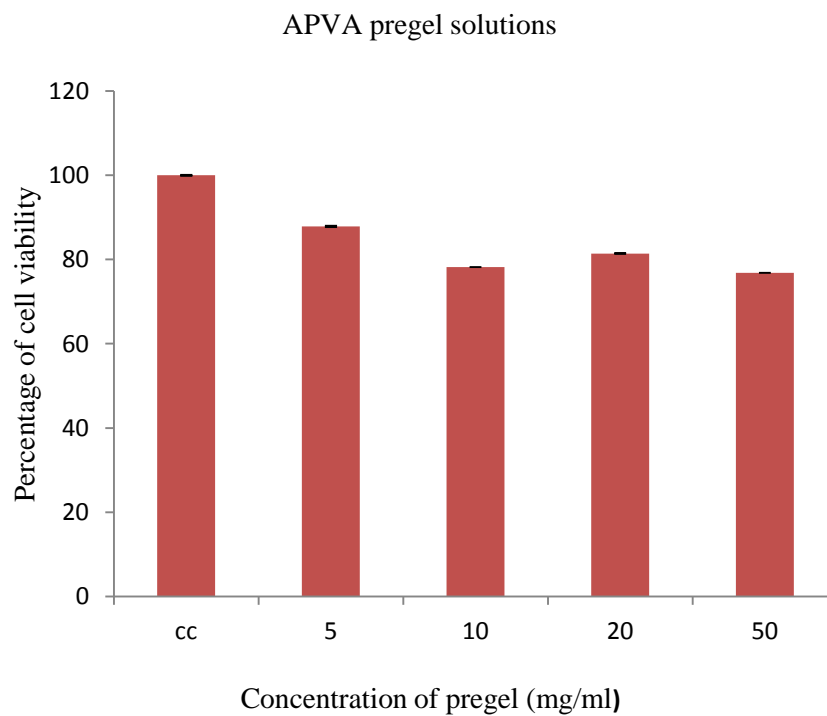
#### ***4.8 In vitro Cytotoxicity***

##### ***4.8.1 MTT Assay of resin***

The cytocompatibility of the pregel formulations were determined using L929 fibroblast cells by MTT assay. Results showed 73% cell viability for OPF pregel formulation having 30 mg/ml concentration whereas APVA pregel formulation having 50 mg/ml concentration showed 76% cell viability (Figure 4.18 and 4.19). These data show that both oligomers showed significant cytocompatibility towards cells in vitro.



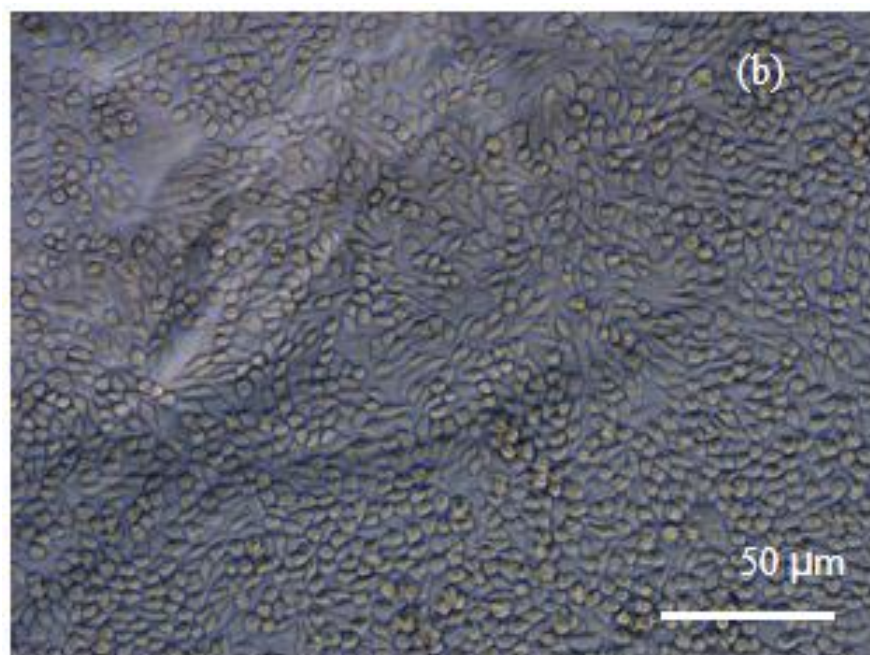
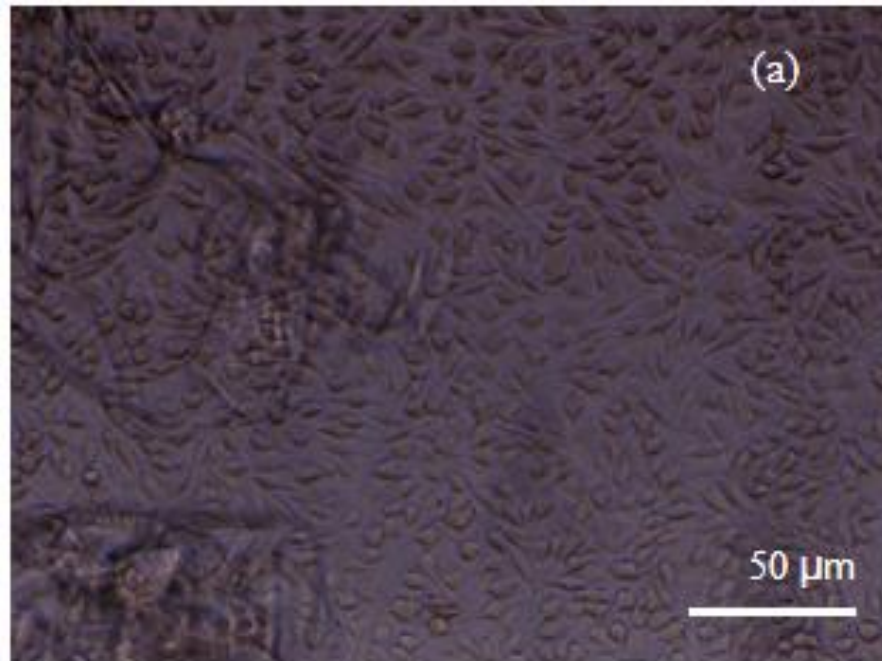
**Figure 4.18. MTT assay of leachable from the OPF pregel solution**

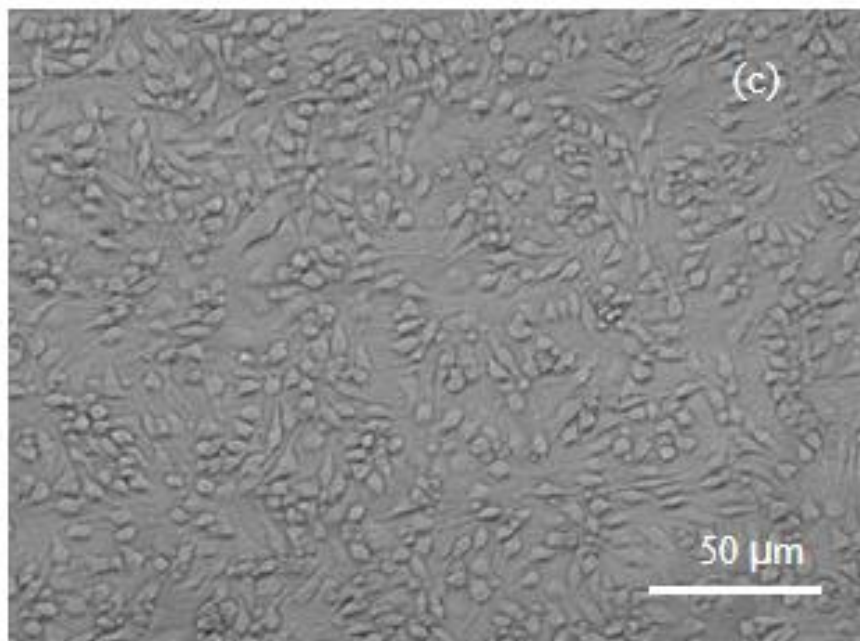


**Figure 4.19. MTT assay of leachable from the APVA pregel solution**

#### 4.8.2. Direct Contact Assay

The direct contact assay of OPFII and APVAII hydrogels on L929 cell monolayers are shown in Figure 4.20. Results demonstrate that the cultured L929 cells did not show any change in cell morphology thereby indicating good cytocompatibility.

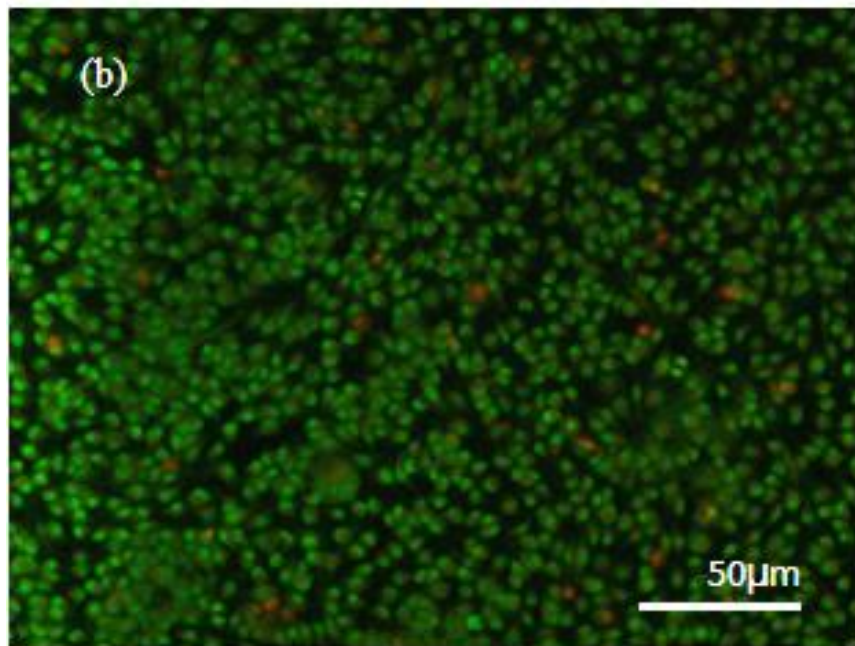
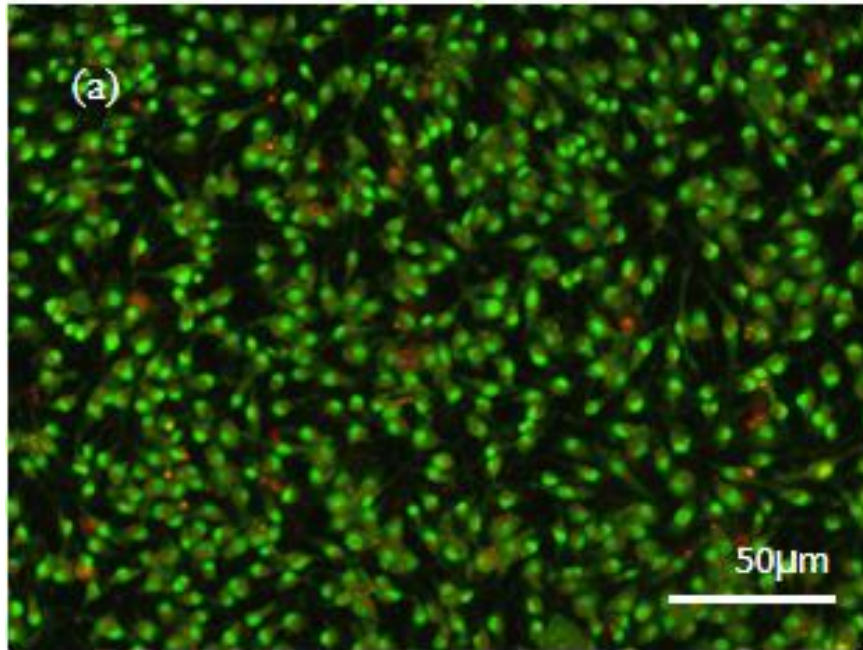




**Figure 4.20. Cytocompatibility- Direct contact assay of hydrogels.**  
**OPFII hydrogel (a), APVAII hydrogel (b) and L929 control cells (c)**

#### *4.8.3. Live/Dead cell Assay*

The cell viability of cells after direct contact with prepared hydrogels was qualitatively assessed by live/dead staining. Acridine orange and the homodimer of ethidium bromide were used to stain live cells (green) and necrotic or apoptotic cells (orange). Figure 4.21 depicts the live dead stain of hydrogels along with cell control. Both OPFII and APVAII hydrogels showed excellent cytocompatibility *in vitro*.



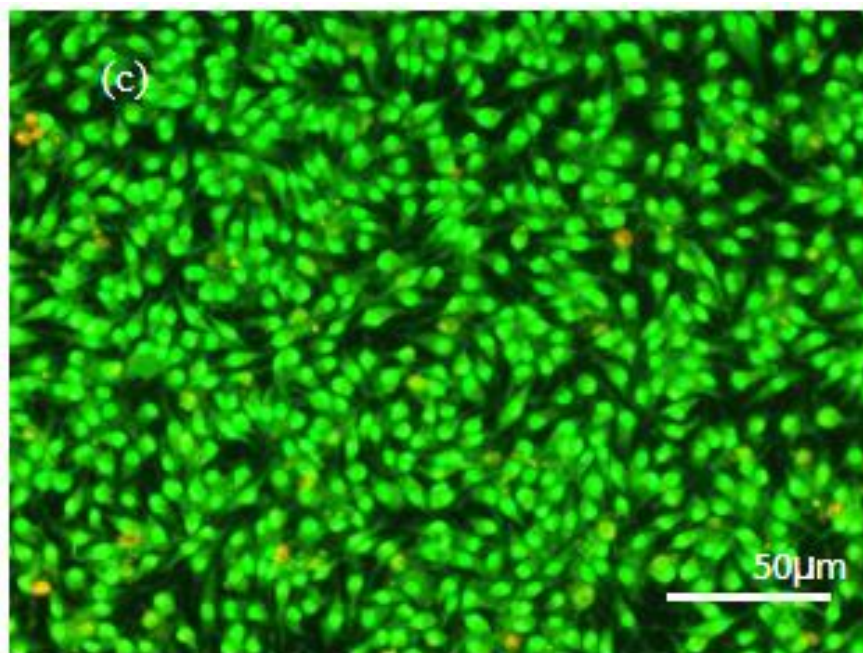


**Figure 4.21. Cell viability of cells on direct contact with hydrogel. OPFII hydrogel (a) , APVAII hydrogels (b) L929 Control cells (c) (Ethidium bromide/Acridine orange staining)**

#### *4.8.4. MTT Assay of hydrogels*

The cytocompatibility of leachable and degradation products of OPFII and APVAII hydrogels were investigated by MTT assay. The studies reveal 80% cell viability for OPFII hydrogel and 100% cell viability for APVAII hydrogel at a high concentration of 10 mg/ml illustrating excellent cytocompatibility in vitro (Figure 4.22 and 4.23).

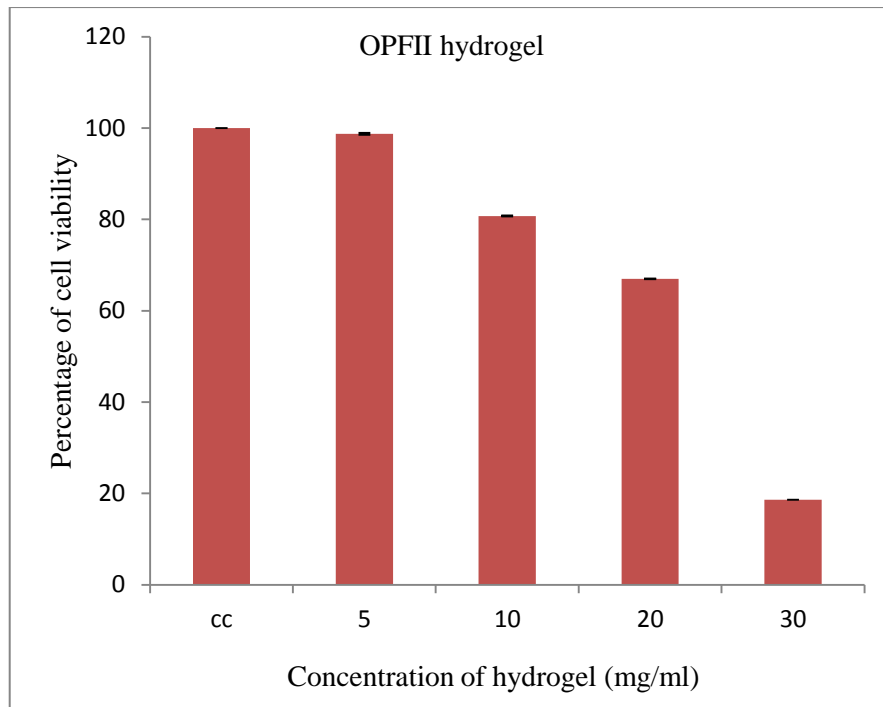


**Figure.4.22. MTT assay of leachables from the OPFII hydrogel**

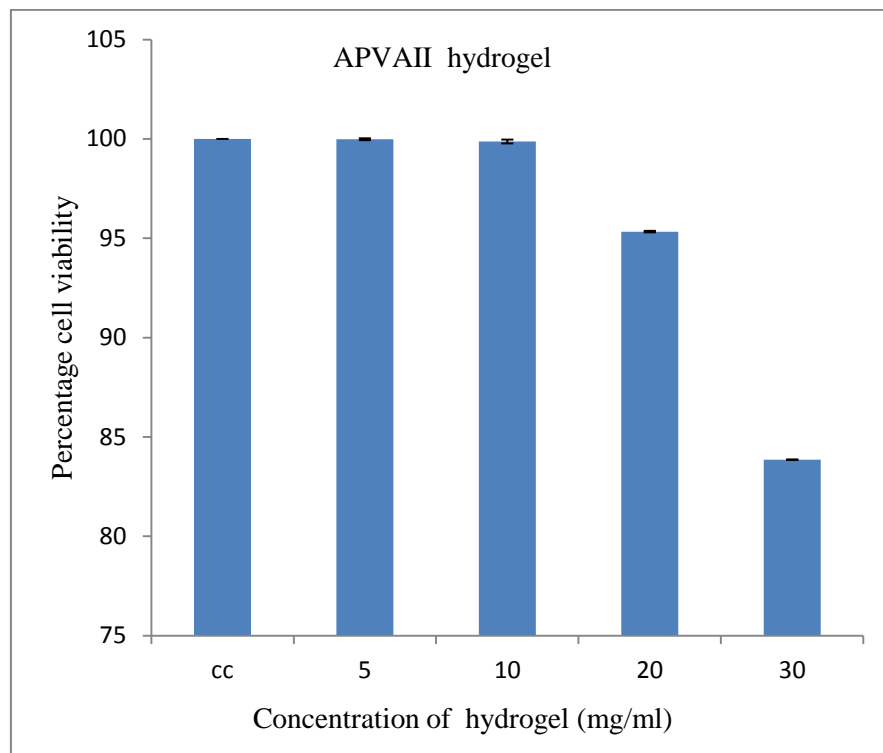


**Figure.4.23. MTT assay of leachables from the APVAII hydrogel**

## Chapter V

### SUMMARY AND CONCLUSION

Vitreous replacement is a challenging and complex problem in clinical ophthalmology. We report syntheses and characterization of in situ cross linkable PEG-based and PVA-based pregel formulation and their comparison for potential use as injectable hydrogel for potential vitreous replacement. Water soluble OPF was synthesized by condensing PEG and fumaryl chloride. In the case of APVA synthesis, the -OH group of PVA underwent a nucleophilic substitution reaction with allyl bromide. The FTIR and  $^1\text{H}$  NMR analyses revealed the formation of OPF resin with functional fumarate groups that can facilitate crosslinks to form a 3-D network. In the case of APVA gels, FTIR and  $^1\text{H}$  NMR confirmed the successful substitution of allyl group into the PVA polymer chain through the presence of double bonds. The determination of molecular weight and polydispersity index of synthesized OPF and APVA via GPC confirmed the oligomer nature.

Polymer hydrogels were prepared using different concentration of PEGDA cross-linker with APS and TEMED as initiators. Both OPF and APVA hydrogels gave the

optimal setting time at RT showing great promise for in situ injectable application. The swelling studies of OPF and APVA hydrogels in water and PBS showed comparatively high swelling in water. The mechanical properties of OPF and APVA hydrogels showed increasing trend of compressive strength and Young's modulus with increasing PEGDA concentration.

Hydrogel degradation studies showed a mass loss of around 60 - 70% for both OPFII and APVAII hydrogels at the end of the 6-week period. ESEM images of hydrogels aged in PBS medium confirmed the presence of interconnecting pores and increase in pore sizes with increase in aging duration. DSC curves of both OPFII and APVAII showed free water content of 67.302% and 73.35% demonstrating the increased hydrophilic character of the both hydrogels. Furthermore, contact angle measurement displayed an angle  $< 75^\circ$  thereby confirming the surface wettability of the hydrogels. In addition, both OPFII and APVAII hydrogels showed a refractive index close to  $\sim 1.33$  which falls close to that of the native vitreous. OPF hydrogels exhibited 15.12 - 70.46% of transmittance whereas APVAII hydrogels showed 44.66 - 74.30% of transmittance in the measured range. The transparency data of these hydrogels is promising for potential use in vitreous application.

The in vitro cytotoxicity of pregel formulations was performed on L929 fibroblast cells. OPF demonstrated 73% cell viability at a high concentration of 30 mg/ml whereas APVA showed 76% cell viability at a high concentration of 50 mg/ml after 24 h incubation. The direct contact assay of both OPFII and APVAII hydrogels showed good cell compatibility with no difference in morphology compared to cell controls after 24 h. Live dead assay on cells after direct contact assay showed very few apoptotic cells for both OPFII and APVAII hydrogels. Furthermore, MTT assay on leachables from prepared hydrogels showed  $> 80\%$  cell viability for OPFII hydrogels and 100% cell viability for APVAII hydrogels at a high concentration of 10 mg/ml.

Taken together, our results show that both PEG-based and PVA-based hydrogels prepared in this work exhibited relevant physical, optical and biological characteristics for use as an in situ forming injectable artificial VS system.

Future studies will aim at employing non-degradable crosslinkers to reduce the degradation of prepared hydrogels thereby prolonging its lifetime which will bring it a step closer towards clinical application as a long-term artificial VS.

## References

1. The Physics of Polymers - Concepts for Understanding Their | Gert R. Strobl | Springer. Available at: <http://www.springer.com/fr/book/9783540252788>. (Accessed: 10th June 2016)
2. Biomaterials A. Binnaz Hazar Yoruç1 and B. Cem Şener2 1Yıldız Technical University, Science and Technology Application and Research Center, 2Marmara University, Faculty of Dentistry, Department of Oral and Maxillofacial Surgery, 57.795j0j8&sourceid=chrome&ie=UTF-8.
3. Polymer Science and Technology - CRC Press Book. Available at: <https://www.crcpress.com/Polymer-Science-and-Technology/Ebewele/p/book/9780849389399>. (Accessed: 10th June 2016)
4. Lyu, S. & Untereker, D. Degradability of Polymers for Implantable Biomedical Devices. *Int. J. Mol. Sci.* **10**, 4033–4065 (2009).
5. Ulery, B. D., Nair, L. S. & Laurencin, C. T. Biomedical Applications of Biodegradable Polymers. *J. Polym. Sci. Part B Polym. Phys.* **49**, 832–864 (2011).
6. Pritchard, C. D. *et al.* Evaluation of viscoelastic poly(ethylene glycol) sols as vitreous substitutes in an experimental vitrectomy model in rabbits. *Acta Biomater.* **7**, 936–943 (2011).
7. Azad, S. V. Vitreous Substitutes. *Delhi J. Ophthalmol.* **23**, 9–13 (2012).
8. Foster, W. J. Vitreous Substitutes. *Expert Rev. Ophthalmol.* **3**, 211–218 (2008).
9. Sebag, J. in *The Vitreous and Vitreoretinal Interface* (eds. M.D, C. L. S. & M.D, A. N.) 37–57 (Springer New York, 1987).
10. Coleman, D. J. Unified model for accommodative mechanism. *Am. J. Ophthalmol.* **69**, 1063–1079 (1970).
11. Sebag, J. Imaging vitreous. *Eye* **16**, 429–439 (2002).

12. Shui, Y.-B. *et al.* The gel state of the vitreous and ascorbate-dependent oxygen consumption: relationship to the etiology of nuclear cataracts. *Arch. Ophthalmol. Chic. Ill 1960* **127**, 475–482 (2009).
13. Hogan, M. J. The vitreous, its structure, and relation to the ciliary body and retina. proctor award lecture. *Invest. Ophthalmol.* **2**, 418–445 (1963).
14. Heegaard, S., Jensen, O. A. & Prause, J. U. Structure and composition of the inner limiting membrane of the retina. SEM on frozen resin-cracked and enzyme-digested retinas of *Macaca mulatta*. *Graefes Arch. Clin. Exp. Ophthalmol. Albrecht Von Graefes Arch. Für Klin. Exp. Ophthalmol.* **224**, 355–360 (1986).
15. Ali, S. & Bettelheim, F. A. Distribution of freezable and non-freezable water in bovine vitreous. *Curr. Eye Res.* **3**, 1233–1239 (1984).
16. Wong, R. W., Richa, D. C., Hahn, P., Green, W. R. & Dunaief, J. L. Iron toxicity as a potential factor in AMD. *Retina Phila. Pa* **27**, 997–1003 (2007).
17. Bos, K. J. *et al.* Axial structure of the heterotypic collagen fibrils of vitreous humour and cartilage. *J. Mol. Biol.* **306**, 1011–1022 (2001).
18. Theocharis, D. A. *et al.* Hyaluronan and chondroitin sulfate proteoglycans in the supramolecular organization of the mammalian vitreous body. *Connect. Tissue Res.* **49**, 124–128 (2008).
19. Reddy, T. S., Birkle, D. L., Packer, A. J., Dobard, P. & Bazan, N. G. Fatty acid composition and arachidonic acid metabolism in vitreous lipids from canine and human eyes. *Curr. Eye Res.* **5**, 441–447 (1986).
20. Sebag, J. Anatomy and pathology of the vitreo-retinal interface. *Eye* **6**, 541–552 (1992).
21. Sebag, J. & Balazs, E. A. Morphology and ultrastructure of human vitreous fibers. *Invest. Ophthalmol. Vis. Sci.* **30**, 1867–1871 (1989).

22. Stay, M. S., Xu, J., Randolph, T. W. & Barocas, V. H. Computer simulation of convective and diffusive transport of controlled-release drugs in the vitreous humor. *Pharm. Res.* **20**, 96–102 (2003).
23. Kleinberg, T. T., Tzekov, R. T., Stein, L., Ravi, N. & Kaushal, S. Vitreous substitutes: a comprehensive review. *Surv. Ophthalmol.* **56**, 300–323 (2011).
24. Nickerson, C. S., Park, J., Kornfield, J. A. & Karageozian, H. Rheological properties of the vitreous and the role of hyaluronic acid. *J. Biomech.* **41**, 1840–1846 (2008).
25. Los, L. I., van der Worp, R. J., van Luyn, M. J. A. & Hooymans, J. M. M. Age-related liquefaction of the human vitreous body: LM and TEM evaluation of the role of proteoglycans and collagen. *Invest. Ophthalmol. Vis. Sci.* **44**, 2828–2833 (2003).
26. Colthurst, M. J., Williams, R. L., Hiscott, P. S. & Grierson, I. Biomaterials used in the posterior segment of the eye. *Biomaterials* **21**, 649–665 (2000).
27. Peyman, G. A., Schulman, J. A. & Sullivan, B. Perfluorocarbon liquids in ophthalmology. *Surv. Ophthalmol.* **39**, 375–395 (1995).
28. Kim, R. W. & Bauman, C. Anterior segment complications related to vitreous substitutes. *Ophthalmol. Clin. N. Am.* **17**, 569–576, vi (2004).
29. Peyman, G. A., Schulman, J. A. & Sullivan, B. Perfluorocarbon liquids in ophthalmology. *Surv. Ophthalmol.* **39**, 375–395 (1995).
30. Orzalesi, N., Migliavacca, L., Bottoni, F. & Miglior, S. Experimental short-term tolerance to perfluorodecalin in the rabbit eye: a histopathological study. *Curr. Eye Res.* **17**, 828–835 (1998).
31. Zeana, D., Becker, J., Kuckelkorn, R. & Kirchhof, B. Perfluorohexyloctane as a long-term vitreous tamponade in the experimental animal. Experimental perfluorohexyloctane substitution. *Int. Ophthalmol.* **23**, 17–24 (1999).

32. Chirila, T. V., Tahija, S., Hong, Y., Vijayasekaran, S. & Constable, I. J. Synthetic polymers as materials for artificial vitreous body: review and recent advances. *J. Biomater. Appl.* **9**, 121–137 (1994).
33. Yu, L. & Ding, J. Injectable hydrogels as unique biomedical materials. *Chem. Soc. Rev.* **37**, 1473–1481 (2008).
34. Zhao, X. Multi-scale Multi-mechanism Design of Tough Hydrogels: Building Dissipation into Stretchy Networks. *Soft Matter* **10**, 672–687 (2014).
35. Tan, H. & Marra, K. G. Injectable, Biodegradable Hydrogels for Tissue Engineering Applications. *Materials* **3**, 1746–1767 (2010).
36. Kurt H. Stenzel, M. W. D. Collagen Gels: Design for a Vitreous Replacement. *Science* **164**, 1282–1283 (1969).
37. Pruett RC, Calabria GA & Schepens CL. Collagen vitreous substitute: I. experimental study. *Arch. Ophthalmol.* **88**, 540–543 (1972).
38. Nakagawa, M., Tanaka, M. & Miyata, T. Evaluation of Collagen Gel and Hyaluronic Acid as Vitreous Substitutes. *Ophthalmic Res.* **29**, 409–420 (1997).
39. Lai, J.-Y. Biocompatibility of chemically cross-linked gelatin hydrogels for ophthalmic use. *J. Mater. Sci. Mater. Med.* **21**, 1899–1911 (2010).
40. Pruett, R. C., Schepens, C. L. & Swann, D. A. Hyaluronic acid vitreous substitute. A six-year clinical evaluation. *Arch. Ophthalmol. Chic. Ill 1960* **97**, 2325–2330 (1979).
41. Suri, S. & Banerjee, R. In vitro evaluation of in situ gels as short term vitreous substitutes. *J. Biomed. Mater. Res. A* **79A**, 650–664 (2006).
42. Baino, F. The Use of Polymers in the Treatment of Retinal Detachment: Current Trends and Future Perspectives. *Polymers* **2**, 286–322 (2010).

43. Cavalieri, F., Miano, F., D'Antona, P. & Paradossi, G. Study of gelling behavior of poly(vinyl alcohol)-methacrylate for potential utilizations in tissue replacement and drug delivery. *Biomacromolecules* **5**, 2439–2446 (2004).
44. Feng, S. *et al.* A Novel Vitreous Substitute of Using a Foldable Capsular Vitreous Body Injected with Polyvinylalcohol Hydrogel. *Sci. Rep.* **3**, (2013).
45. Davidorf, F. H. *et al.* Ocular toxicity of vitreal pluronic polyol F-127. *Retina Phila. Pa* **10**, 297–300 (1990).
46. Katagiri, Y. *et al.* Application of thermo-setting gel as artificial vitreous. *Jpn. J. Ophthalmol.* **49**, 491–496 (2005).
47. Su, X. *et al.* Recent Progress in Using Biomaterials as Vitreous Substitutes. *Biomacromolecules* **16**, 3093–3102 (2015).
48. Lirong He, D. S. Toward Self-Healing Hydrogels Using One-Pot Thiol–Ene Click and Borax-Diol Chemistry. *ACS Macro Lett.* **4**, 673–678 (2015).
49. Wang, S., Lu, L., Gruetzmacher, J. A., Currier, B. L. & Yaszemski, M. J. Synthesis and characterizations of biodegradable and crosslinkable poly(epsilon-caprolactone fumarate), poly(ethylene glycol fumarate), and their amphiphilic copolymer. *Biomaterials* **27**, 832–841 (2006).
50. Krishna, L. & Jayabalan, M. Synthesis and characterization of biodegradable poly (ethylene glycol) and poly (caprolactone diol) end capped poly (propylene fumarate) cross linked amphiphilic hydrogel as tissue engineering scaffold material. *J. Mater. Sci. Mater. Med.* **20**, 115–122 (2008).
51. Shin, H., Temenoff, J. S. & Mikos, A. G. In vitro cytotoxicity of unsaturated oligo[poly(ethylene glycol) fumarate] macromers and their cross-linked hydrogels. *Biomacromolecules* **4**, 552–560 (2003).

52. Kuo, S.-M., Liou, C.-C., Chuang, C.-L. & Wang, Y.-J. Studies of the effects of PVA-AE on dentinal bonding of HEMA. *ResearchGate* **21**, (2001).
53. Kuo, S. M., Liou, C. C., Chang, S. J. & Wang, Y.-J. Synthesis and characterizations of hydrogel based on PVA-AE and HEMA. *J. Polym. Res.* **8**, 169–174 (2001).
54. Kinard, L. A., Kasper, F. K. & Mikos, A. G. Synthesis of oligo(poly(ethylene glycol) fumarate). *Nat. Protoc.* **7**, 1219–1227 (2012).
55. Balakrishnan, B., Mohanty, M., Umashankar, P. R. & Jayakrishnan, A. Evaluation of an in situ forming hydrogel wound dressing based on oxidized alginate and gelatin. *Biomaterials* **26**, 6335–6342 (2005).
56. Qi, X. *et al.* Investigation of Salecan/poly(vinyl alcohol) hydrogels prepared by freeze/thaw method. *Carbohydr. Polym.* **118**, 60–69 (2015).
57. Yudianti, R., Karina, M., Sakamoto, M. & Azuma, J. DSC analysis on water state of salvia hydrogels. *Macromol. Res.* **17**, 1015–1020 (2009).
58. Gustafson, C. T. *et al.* Controlled Delivery of Vancomycin via Charged Hydrogels. *PLoS ONE* **11**, (2016).
59. Mbhele, Z. H. *et al.* Fabrication and Characterization of Silver–Polyvinyl Alcohol Nanocomposites. *Chem. Mater.* **15**, 5019–5024 (2003).
60. Baino, F. Towards an ideal biomaterial for vitreous replacement: Historical overview and future trends. *Acta Biomater.* **7**, 921–935 (2011).